Recent results on hard and rare probes from ATLAS

Mariusz Przybycień

AGH University of Science and Technology, Krakow, Poland

(on behalf of the ATLAS Collaboration)

Motivation and recent ATLAS results

- QGP exists for a short time ($t \sim 10$ fm/$c \sim 10^{-23}$ s) – need a probe from inside the collision region.

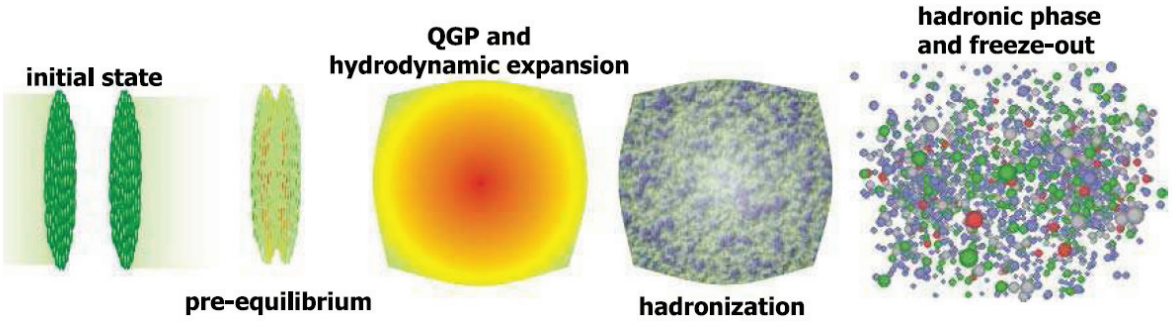

- Hard probes are produced early in the HI collision, in a process which cross section is not changed by presence of strongly interacting medium, i.e. can by calculated in pQCD.
- Passing through the medium hard probes interact weakly or strongly with it providing information on its properties.

The following measurements will be reviewed in this talk:

- Measurement of angular and momentum distributions of charged particles within and around jets in Pb+Pb and pp collisions at $\sqrt{s_{\mathrm{NN}}} = 5.02$ TeV with the ATLAS detector. Phys. Rev. C 100, 064901 (2019)
- Measurement of suppression of large-radius jets and its dependence on substructure in Pb+Pb at 5.02 TeV with the ATLAS detector. ATLAS-CONF-2019-056
- Measurement of $W^{\pm}$ boson production in Pb+Pb collisions at $\sqrt{s_{\mathrm{NN}}} = 5.02$ TeV with the ATLAS detector. Eur. Phys. J. C 79, 935 (2019)
- Z boson production in Pb+Pb collisions at $\sqrt{s_{\mathrm{NN}}} = 5.02$ TeV measured by the ATLAS experiment. Phys. Lett. B 802, 135262 (2020)
- Measurement of light-by-light scattering and search for axion-like particles with 2.2 nb^{-1} of Pb+Pb data with the ATLAS detector. ATLAS-CONF-2020-010

Jets as probes of the Quark-Gluon Plasma

- High transverse momentum partons, produced in hard scattering process, propagating through the medium of strongly interacting nuclear matter, lose energy, resulting in the phenomenon of 'jet quenching'.
- Magnitude of the suppresion is expected to depend on both the p_{T} dependence of energy loss as well as the shape of initial jet p_{T} spectrum.
- Nuclear modification factor: $$R_{\mathrm{AA}} = \frac{1}{N_{\mathrm{evt}}} \frac{1}{\langle T_{\mathrm{AA}} \rangle} \left(\frac{d^2 N_{\mathrm{proc}}}{dp_{\mathrm{T}} dy} \bigg|_{\mathrm{cent}} \right) \Big/ \frac{d^2 \sigma^{pp}_{\mathrm{proc}}}{dp_{\mathrm{T}} dy}$$
- A continuous suppression of jet production from peripheral to central Pb+Pb collisions with respect to pp reference is observed.
- R_{AA} is observed to grow slowly (quenching decreases) with increasing jet p_{T}.

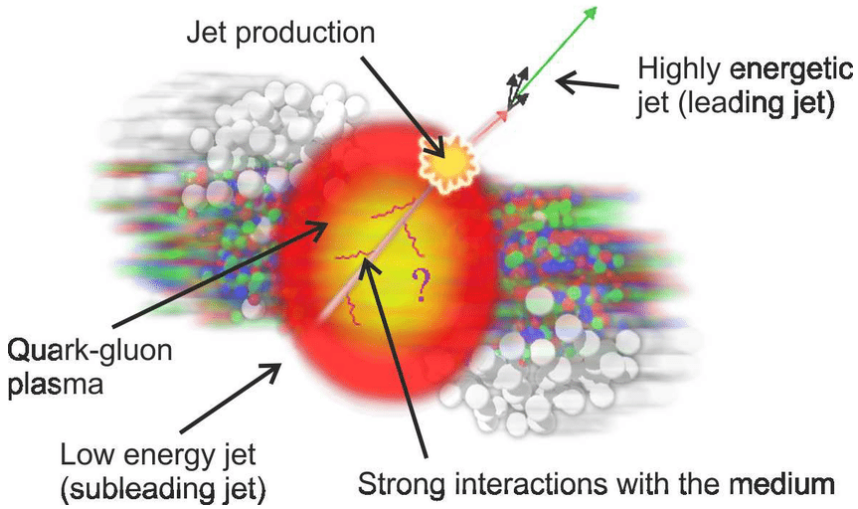

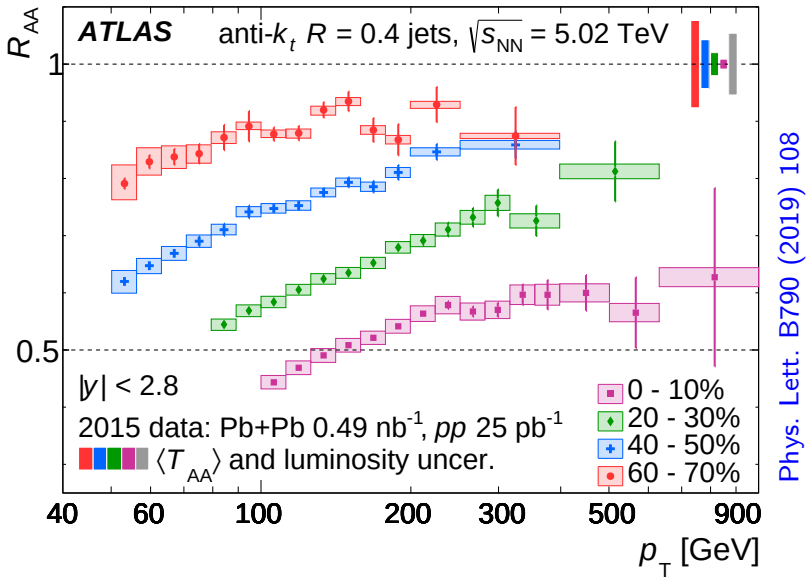

Charged-particle distributions within and around jet

- Yields of charged-particles as a function of particle's p_{T} and distance r from the jet axis:

$$D(p_{\mathrm{T}}, r) = \frac{1}{N_{\mathrm{jet}}} \frac{1}{2\pi r\, dr} \frac{dn_{\mathrm{ch}}(p_{\mathrm{T}}, r)}{dp_{\mathrm{T}}}$$

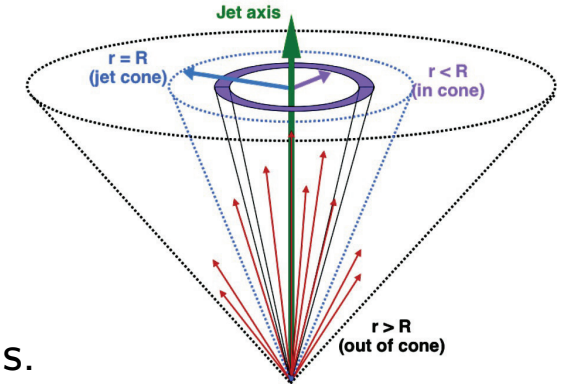

- D(p_{T}, r) decrease as a function of distance from the jet axis.
- The rate of fall-off increases sharply for higher p_{T} particles, with most of these being concentrated near the jet axis.
- The distributions exhibit a difference in shape between Pb+Pb and pp collisions, with the Pb+Pb distributions being broader at low p_{T} and narrower at high p_{T}.

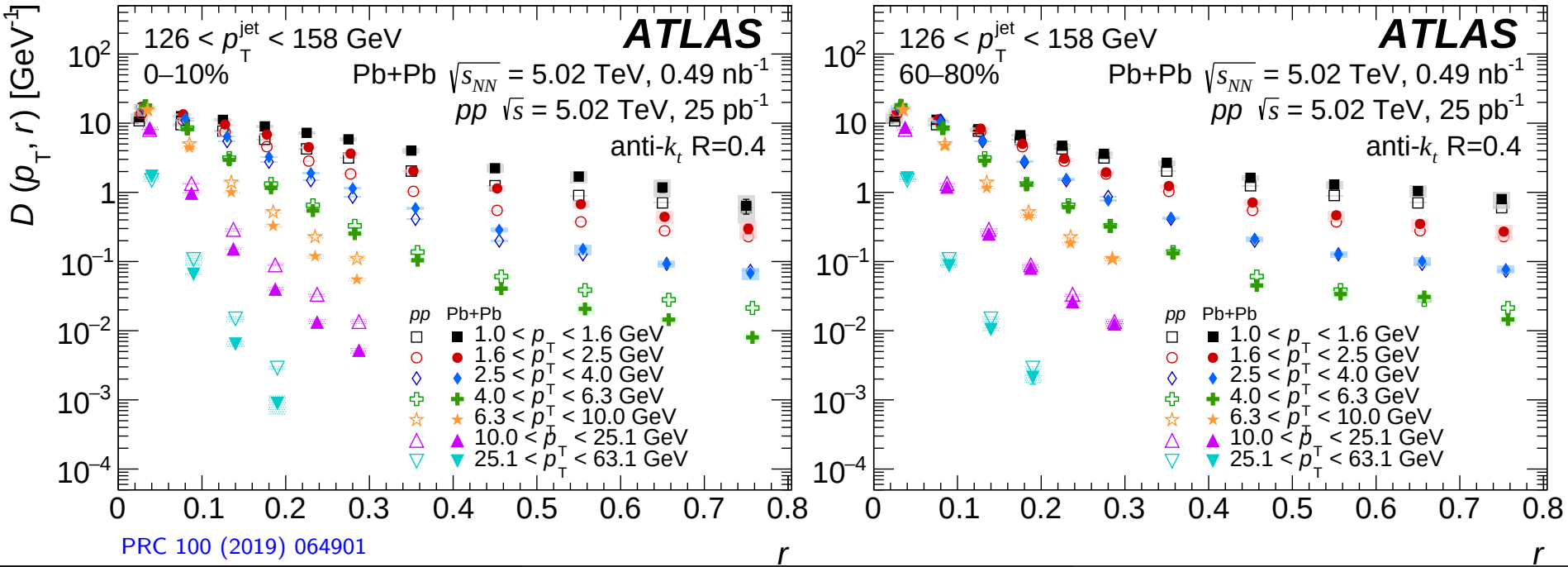

PRC 100 (2019) 064901

Ratio of charged-particle yields in Pb+Pb and pp collisions

- Use the observable $R_{D(p_{\mathrm{T}},r)} = D(p_{\mathrm{T}},r)_{\mathrm{Pb+Pb}} \big/ D(p_{\mathrm{T}},r)_{pp}$ to quantify modifications of the yields due to the QGP.
- $R_{D(p_{\mathrm{T}},r)}$ is shown as a function of r for different p_{T} and centrality ranges for jets with $126 < p_{\mathrm{T}}^{\mathrm{jet}} < 158$ GeV.
- Central and midcentral collisions: $R_{D(p_{\mathrm{T}},r)} > 1$ for particles with $p_{\mathrm{T}} < 4$ GeV, and (for $r > 0.05$) shows a depletion for particles with $p_{\mathrm{T}} > 4$ GeV.
- Peripheral collisions: no significant r-dependence. (not shown)
- Closer look at centrality dependence: Magnitude of the excess or suppresion increase for more central events in both p_{T} intervals.

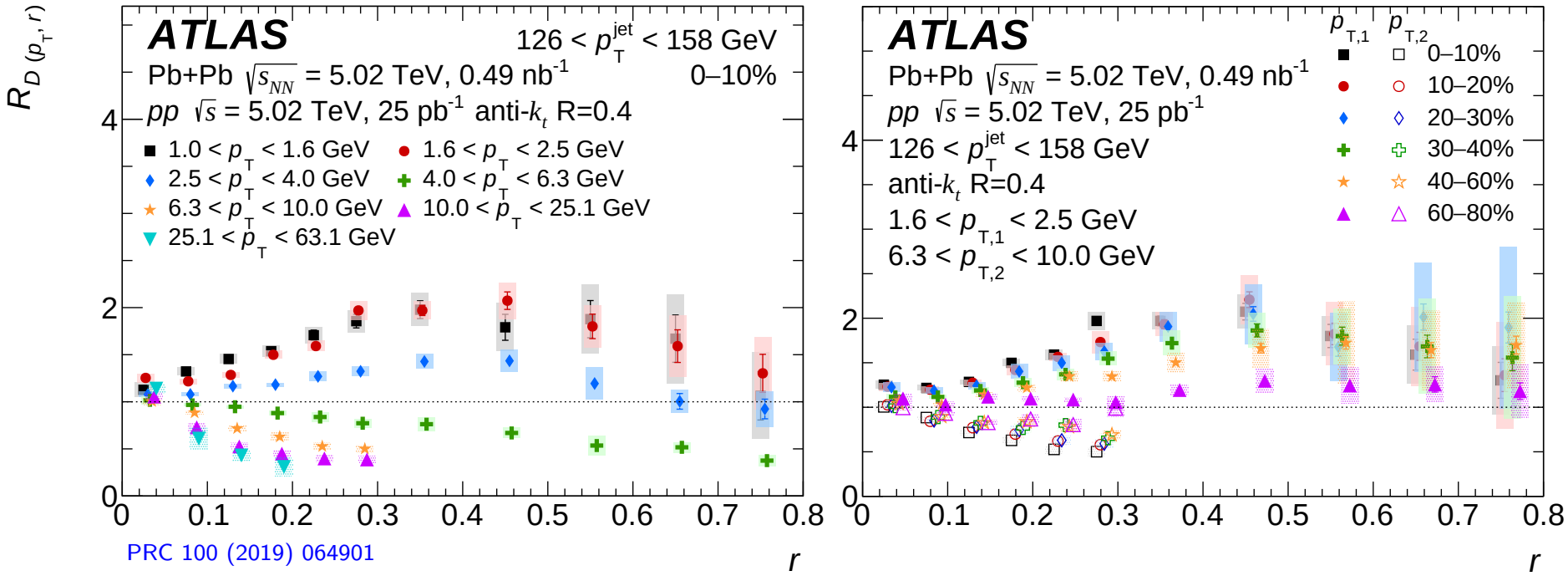

Difference vs. ratio of charged-particle yields

- The difference of the charged-particle yields measured in Pb+Pb and pp collisions:

$$\Delta D(p_{\mathrm{T}}, r) = D(p_{\mathrm{T}}, r)_{\mathrm{Pb+Pb}} - D(p_{\mathrm{T}}, r)_{pp}$$

  quantifies modifications of the yields due to the QGP in terms of particle density (per unit area per GeV).

- An excess in the charged-particle yield density for Pb+Pb collisions compared to pp collisions is observed for charged particles with $p_{\mathrm{T}} < 4$ GeV, mainly within the jet cone.

- This behaviour is different to the ratios $R_{D(p_{\mathrm{T}},r)}$ where the biggest excess is observed at large r due to the fact that the pp signal is small there.

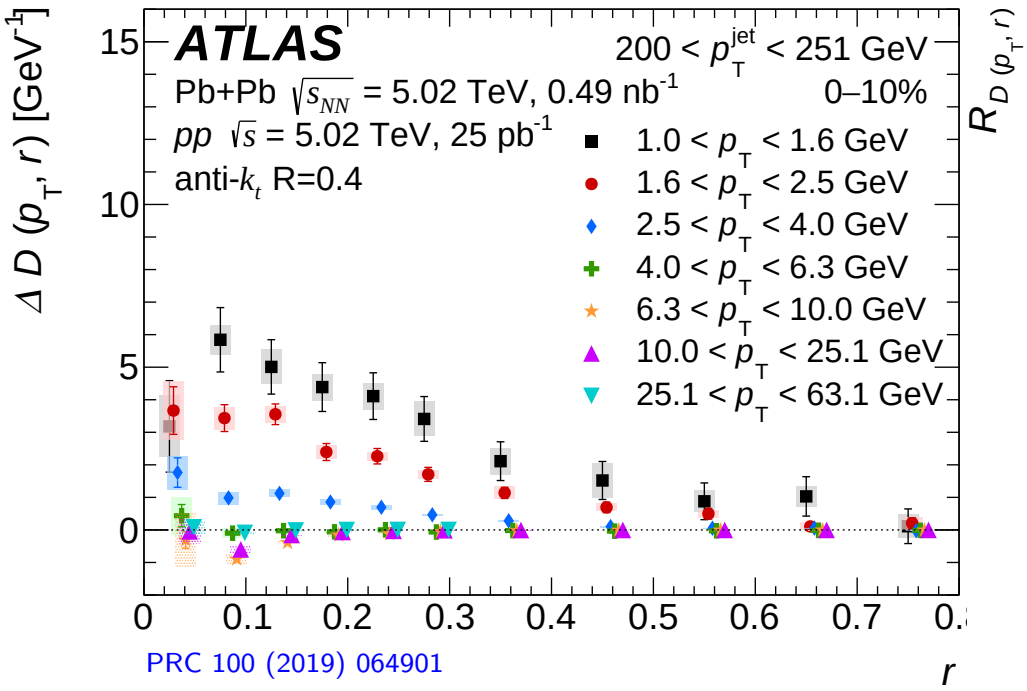

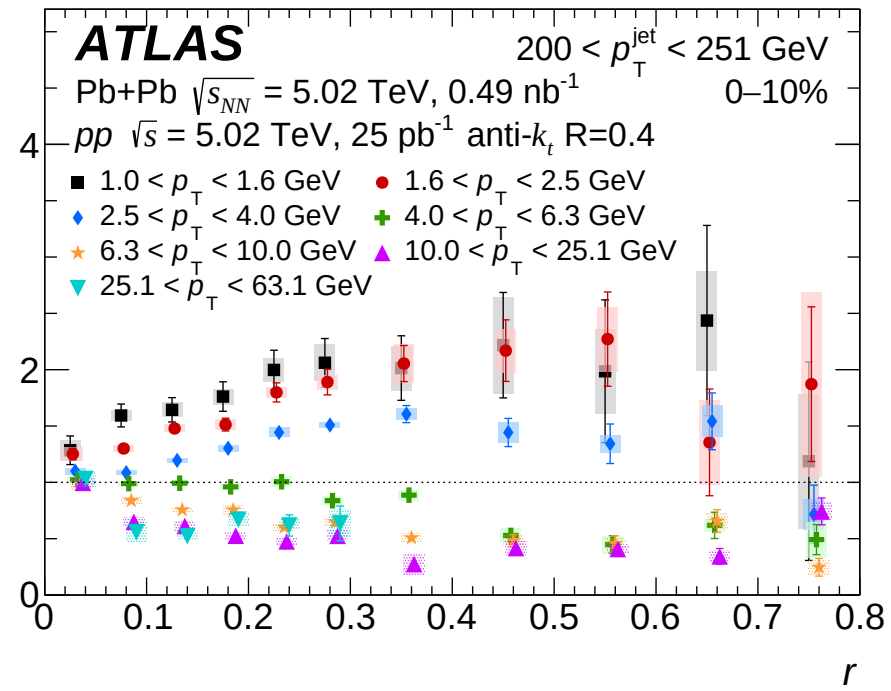

Suppression of large-radius jets

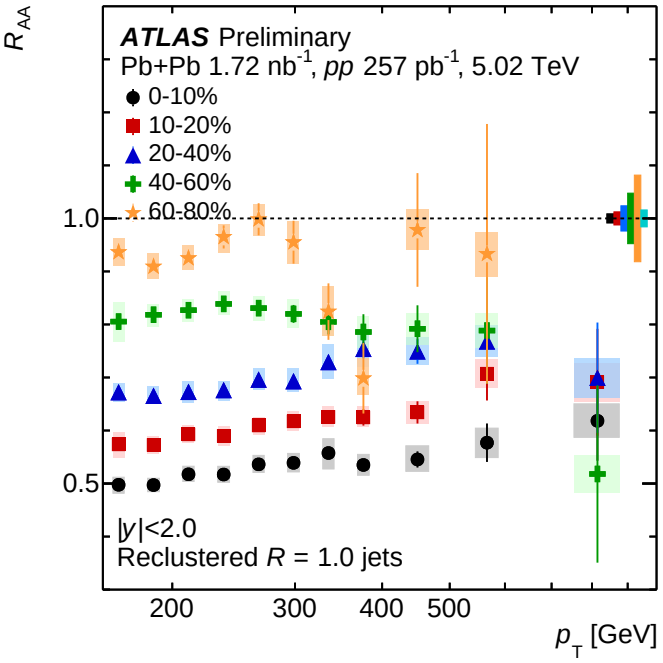

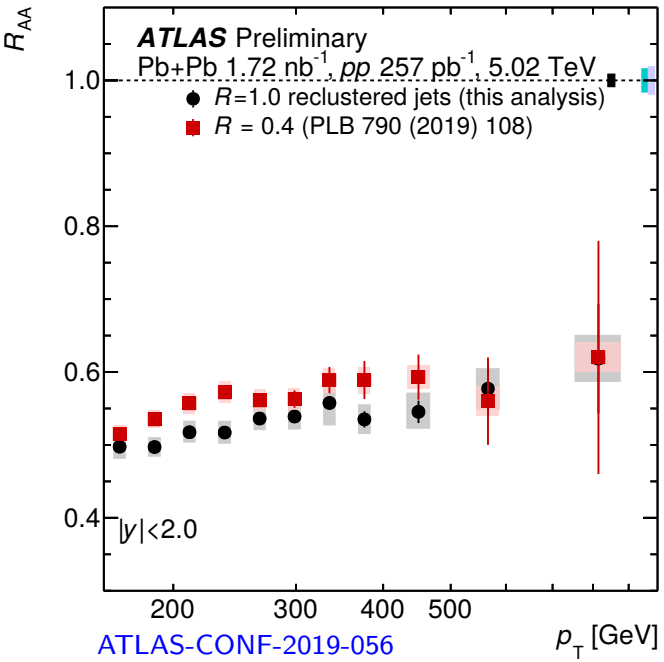

ATLAS-CONF-2019-056

- Large-radius jets ($R = 1$) are obtained by reclusterring small-radius ($R = 0.2$) jets with $p_{\mathrm{T}}^{\mathrm{jet}} > 35$ GeV.
- For re-clustered jets the energy radiated between the $R = 0.2$ sub-jets is removed and lost energy is not recovered, so (re-clustered $R = 1$ jets) $\neq$ ($R = 1$ jets)
- Distance definition:

$$d_{ij} = \min(p_{\mathrm{T},i}^2, p_{\mathrm{T},j}^2) \cdot \Delta R_{ij}^2, \quad \Delta R_{ij} = \sqrt{\Delta\phi_{ij}^2 + \Delta y_{ij}^2}$$

- Nuclear modification factor:

$$R_{\mathrm{AA}} = \frac{1}{N_{\mathrm{evt}}} \frac{1}{\langle T_{\mathrm{AA}} \rangle} \left(\frac{d^3 N_{\mathrm{jet}}}{dp_{\mathrm{T}} d\sqrt{d_{12}} dy} \bigg|_{\mathrm{cent}} \right) \Big/ \frac{d^3 \sigma_{\mathrm{jet}}^{pp}}{dp_{\mathrm{T}} d\sqrt{d_{12}} dy}$$

d_{12} referes to the two jets before the final clustering step in the anti-k_t jet finding algorithm.

- Clear suppression of large-radius jet production in central collisions.
- The magnitude of the R_{AA} is lower for large-radius jets than for small-radius jets.

Suppression of large-radius jets

- d_{12} referes to the two jets before the final clustering step in the anti-k_t jet finding algorithm, corresponding to the hardest splitting in the jet, so it characterizes the jet substructure scale. For jets with only a single sub-jet (SSJ) $d_{12} = 0$.
- Significantly different values of R_{AA} for SSJ compared to jets with multiple sub-jets.
- The SSJ jets are less suppressed with respect to those with higher sub-jet multiplicity.
- Continous increase of the suppression with increasing centrality.
- For SSJ jets, R_{AA} grows slowly with increasing jet p_{T}.
- No significant p_{T} dependence of R_{AA} is seen for jets with multiple sub-jets. (not shown)

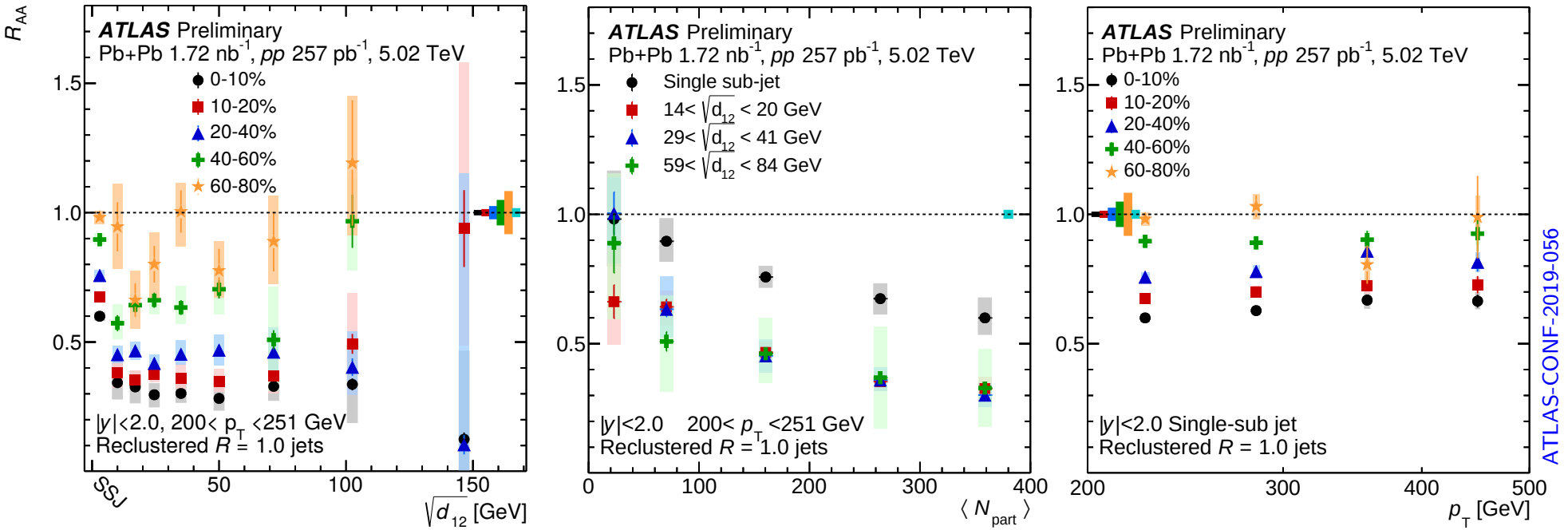

Probing QGP with electroweak bosons

- Electroweak (EW) bosons and their leptonic decay products do not interact strongly. Therefore if formed in a hard parton-parton interaction at a very early stage of the Pb+Pb collision they carry out unmodified information about the geometry of the nuclei at the collision time.
- In LO, $W^+(W^-)$ bosons are produced by interactions of $u(d)$ valence quarks and $\bar{d}(\bar{u})$ sea quarks.
- Z and W boson production yields per binary collision do not depend on centrality. This is consistent with a view of heavy ion collisions as a superposition of binary nucleon-nucleon collisions.

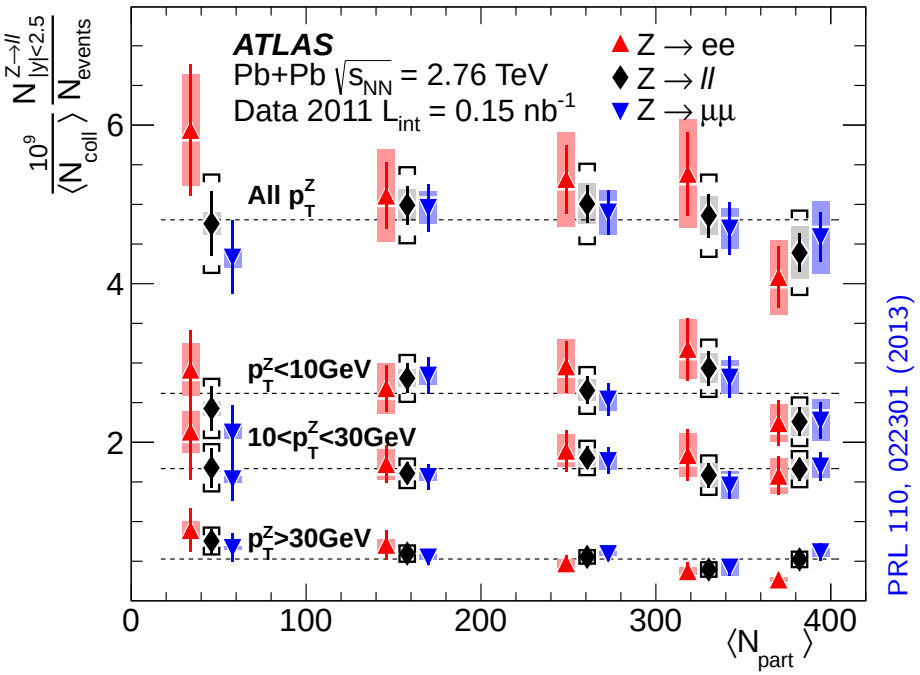

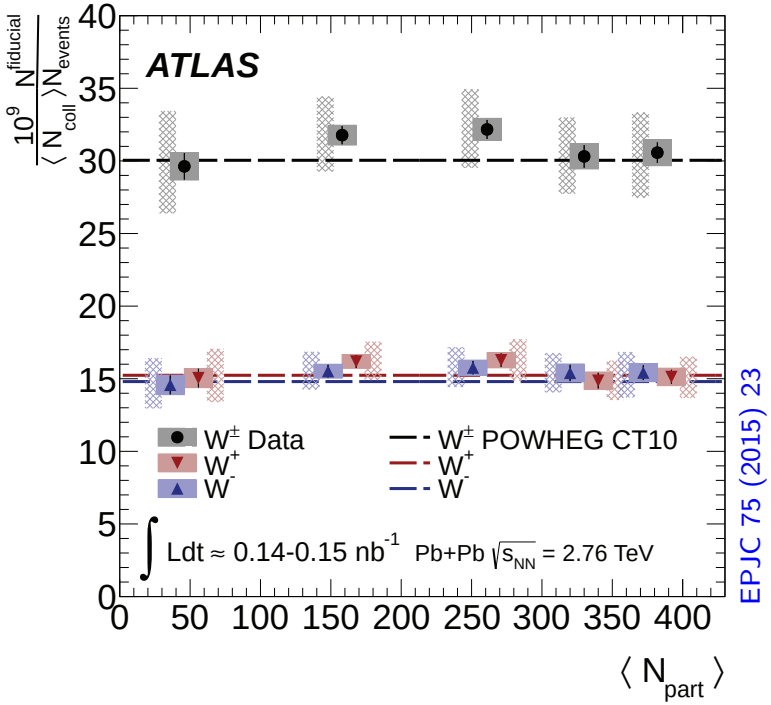

W/Z boson yields in Pb+Pb collisions at $\sqrt{s_{\mathrm{NN}}} = 5.02$ TeV

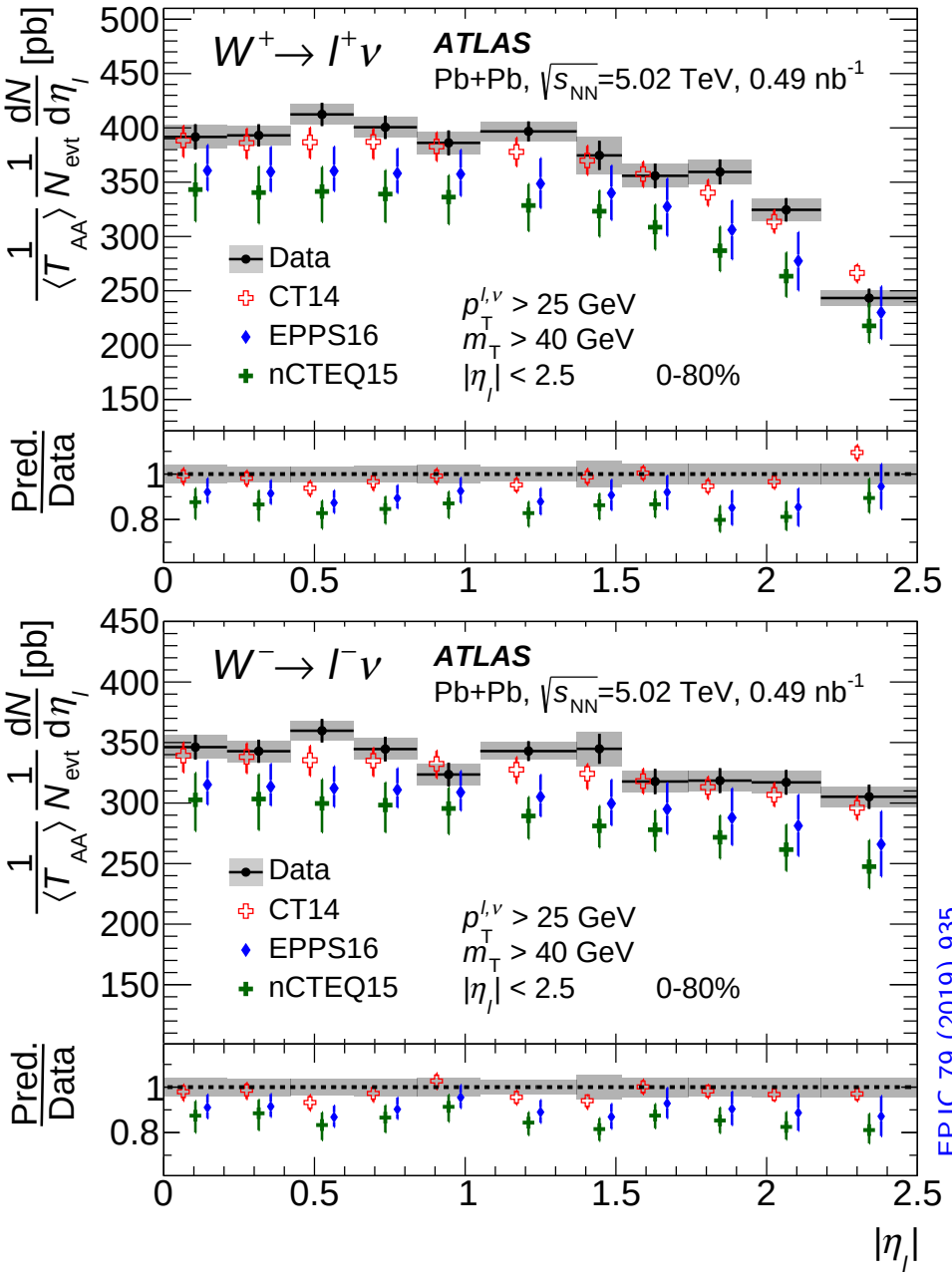

EPJC 79 (2019) 935

- Combined measurements in electron and muon decay channels.
- Normalized $W^{\pm}/Z$ boson yields as function of $|\eta_\ell|/y$, integrated over centrality, are compared with free proton PDF (+isospin) and nPDFs.
- All predictions describe the shapes well, but the normalisation is underestimated by nPDFs (10-20%).

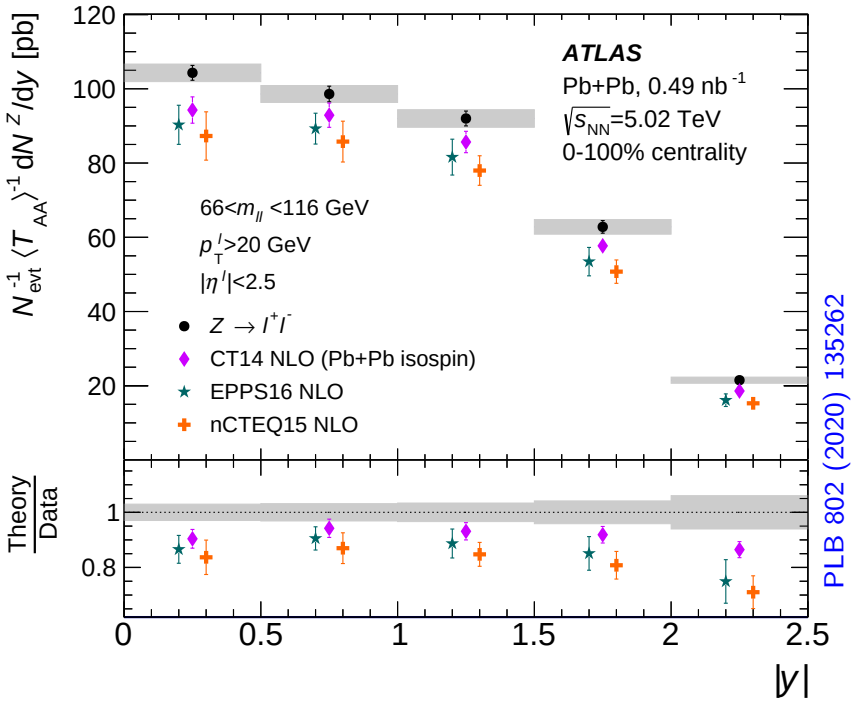

PLB 802 (2020) 135262

W/Z boson yields in Pb+Pb collisions at $\sqrt{s_{\mathrm{NN}}} = 5.02$ TeV

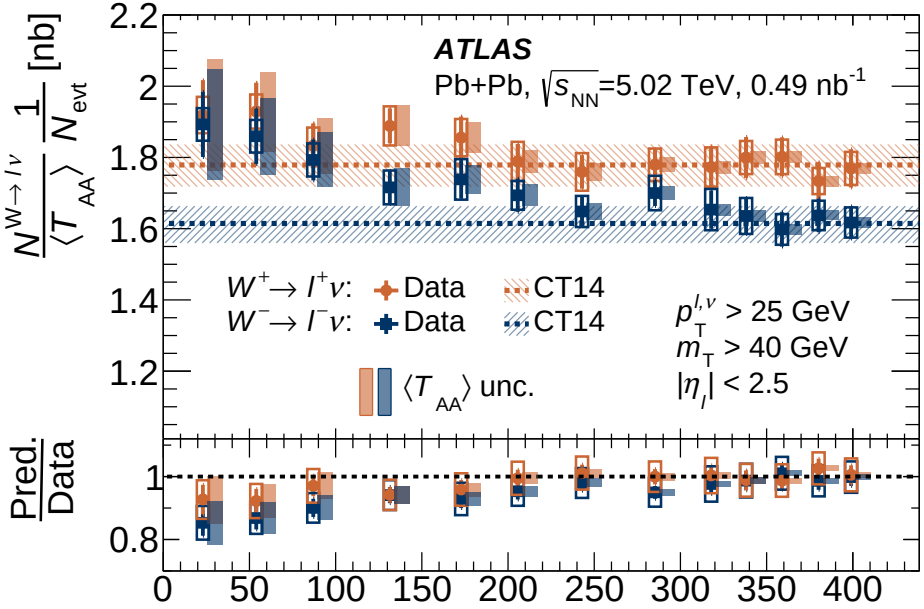

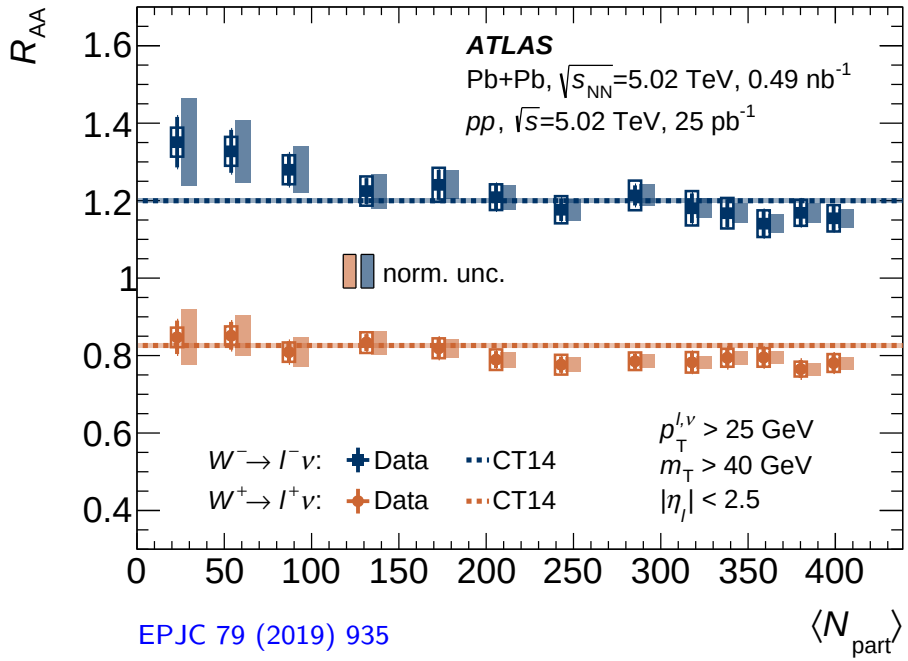

EPJC 79 (2019) 935

- Normalized $W^{\pm}$ boson yields as function of $\langle N_{\mathrm{part}} \rangle$ are in good agreement with theory predictions for $\langle N_{\mathrm{part}} \rangle > 200$, but a slight excess of the data over predictions in more peripheral collisions is observed.
- Normalized Z boson yields consistent with the pp cross-section at all centralities and show only weak dependence on $\langle N_{\mathrm{part}} \rangle$.
- These are also reflected in R_{AA} behaviour.

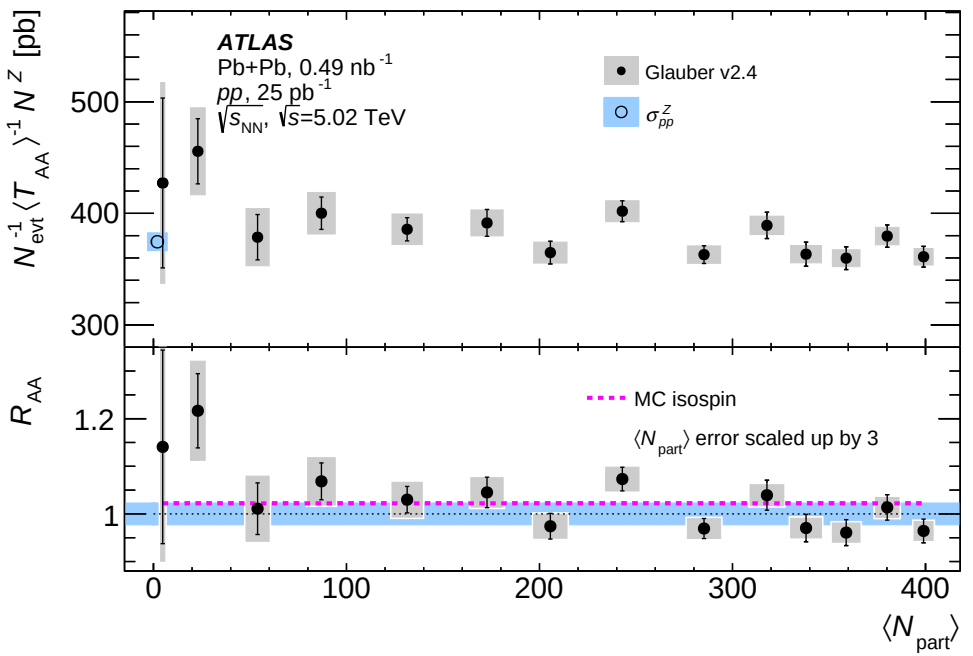

PLB 802 (2020) 135262

Possible shadowing in inelastic nucleon-nucleon cross section

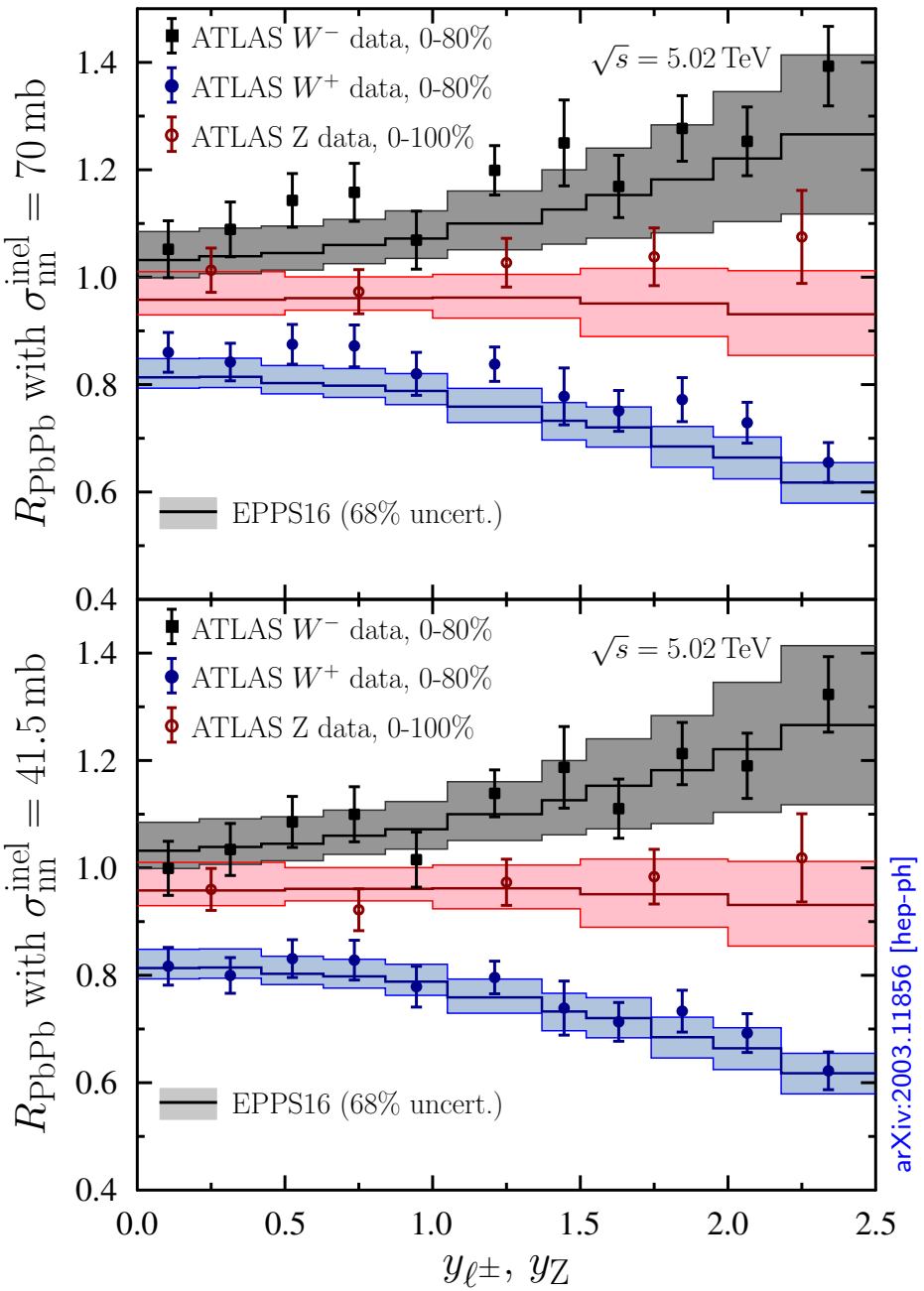

- Measurements of EW bosons production in HI collisions depend on normalisations from the Glauber model calculations, where the inelastic nucleon-nucleon cross section, $\sigma_{nn}^{\mathrm{inel}}$, is taken from pp measuremnets, $\sigma_{pp}^{\mathrm{inel}} = 70\,\mathrm{mb}$.
- Gluon shadowing and saturation phenomena at small x, might be more pronounced in HI collisions, especially at high energies, and as a result the $\sigma_{nn}^{\mathrm{inel}}$ might be reduced.
- Recently K. Eskola et al. (arXiv:2003.11856 [hep-ph]) suggested to treat the EW bosons as "standard candles" and used the ATLAS data to obtain a new value of $\sigma_{nn}^{\mathrm{inel}}$.
- Using EPPS16 and NNPDF3.1 (+MCFM) they obtained theory predictions for R_{AA}. By comparing it with the measured R_{AA} vs. η_ℓ or y_Z it is possible to convert each data point to a new value for $\langle T_{\mathrm{AA}} \rangle$, which via the Glauber MC are directly related to $\sigma_{nn}^{\mathrm{inel}}$.
- New value from the fit: $\sigma_{nn}^{\mathrm{inel}} = 41.5^{+16.2}_{-12.0}\,\mathrm{mb}$

Possible shadowing in inelastic nucleon-nucleon cross section

- Significant change of $\sigma_{nn}^{\mathrm{inel}}$ leads to a rather modest change of $\langle T_{\mathrm{AA}} \rangle$ in central events. The impact grows towards more peripheral centrality classes, where also other effects such as possible centrality dependence of $\sigma_{nn}^{\mathrm{inel}}$ or the neutron-skin effect may become important to explain the data behaviour.

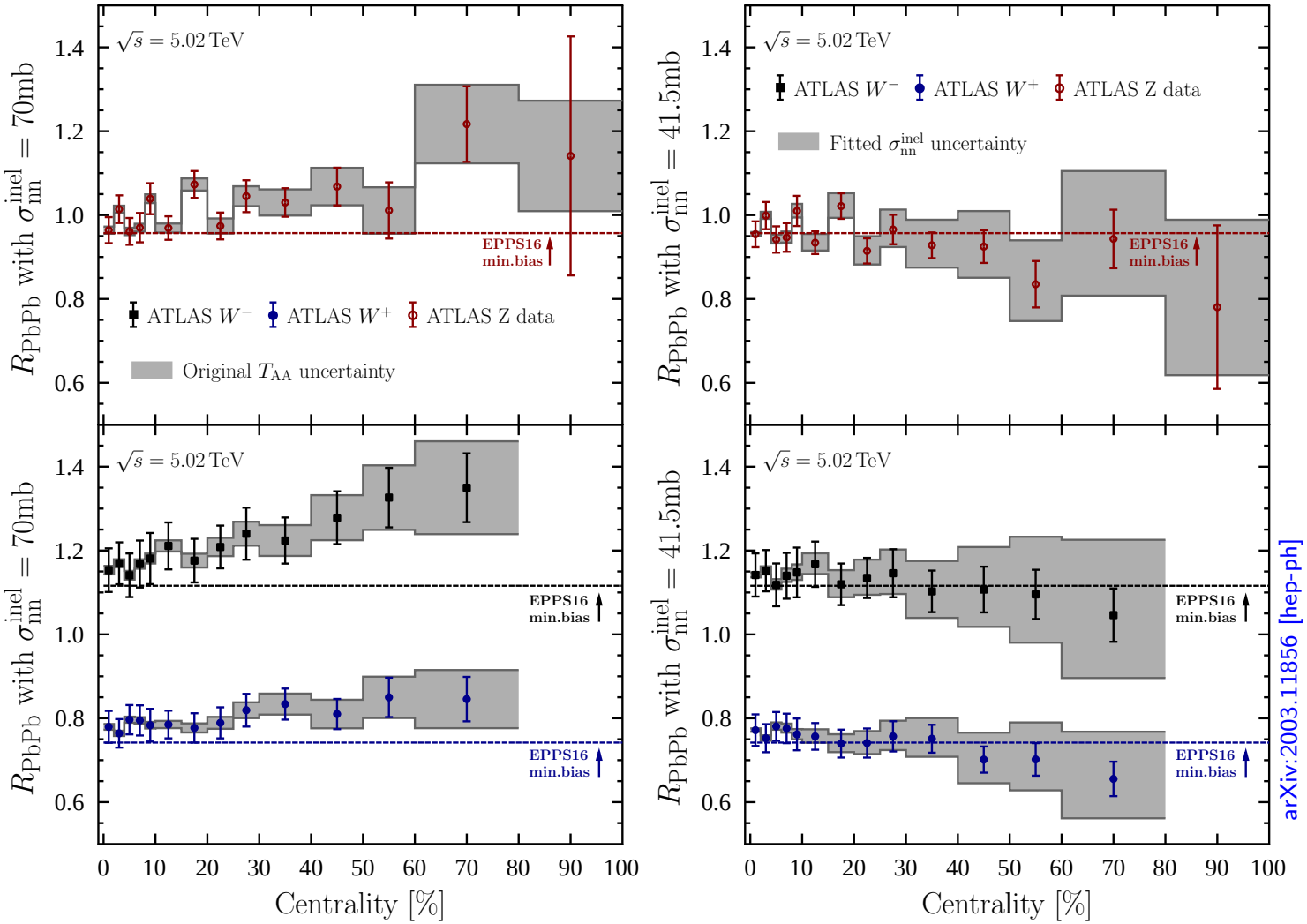

Axion-like particles in light-by-light scattering

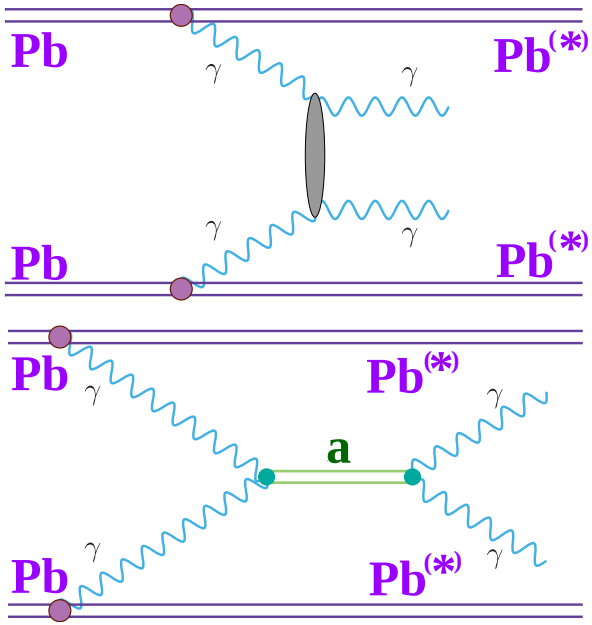

- Measured fiducial cross section ($p_{\mathrm{T}}^{\gamma} > 2.5$ GeV, $|\eta_{\gamma}| < 2.4$, $m_{\gamma\gamma} > 5$ GeV, $p_{\mathrm{T}}^{\gamma\gamma} < 1$ GeV, Aco < 0.01): $\sigma_{\mathrm{fid}} = 120 \pm 17\,(\mathrm{stat}) \pm 13\,(\mathrm{sys}) \pm 4\,(\mathrm{lumi})$ nb
- The measured diphoton invariant mass is used to set upper limits at the 95% CL on the ALP production cross section in the process $\gamma\gamma \rightarrow a \rightarrow \gamma\gamma$ and also on the ALP coupling to photons $(1/\Lambda_a)$.
- Best exclusion limits so far over the mass range of $6 < m_a < 100$ GeV.

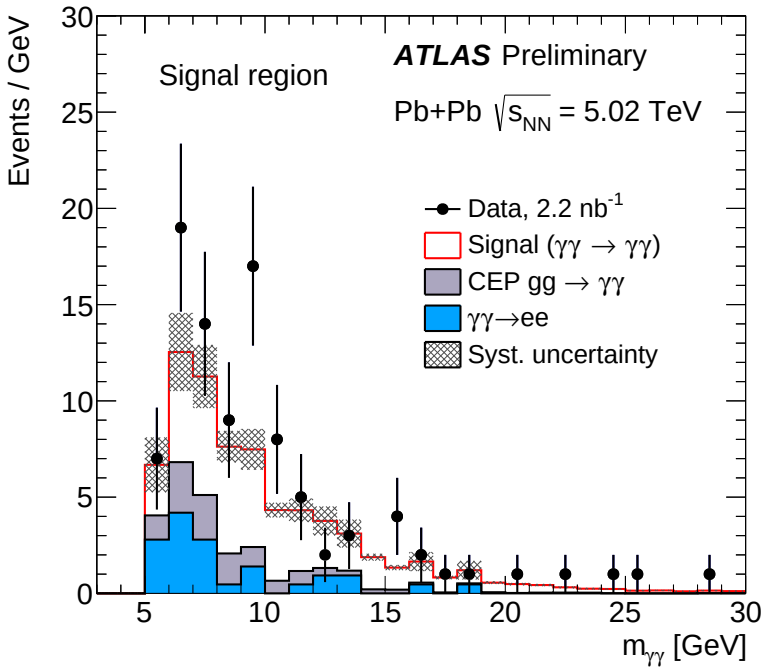

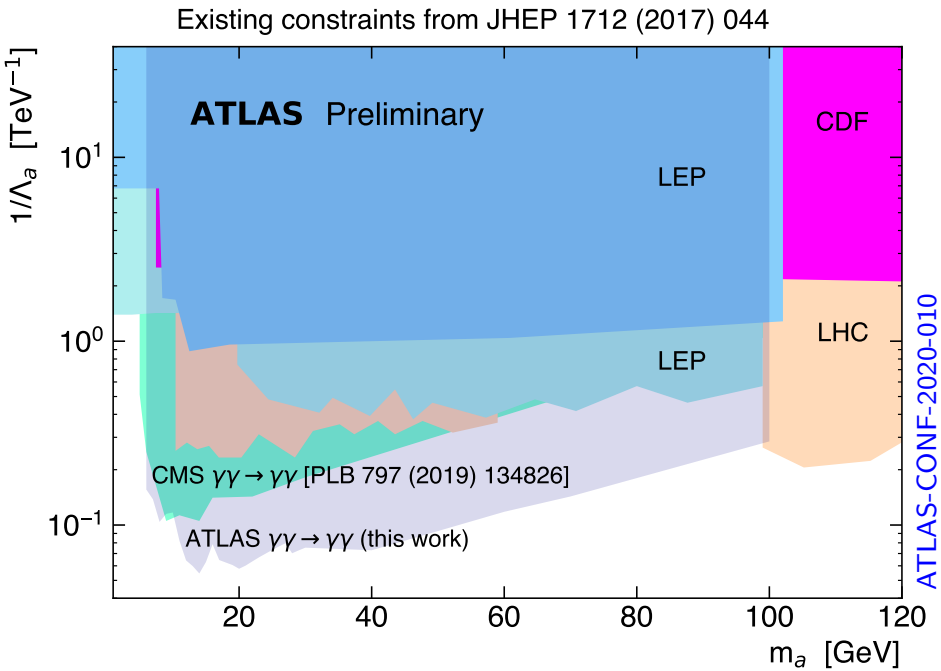

Summary

- Detailed study of the yields of charged-particles inside and around jets in Pb+Pb and pp collisions provided information about the modification of the jet at large distances from the jet axis that can be used to constrain models of how the jet is modified by the presence of the QGP and how the QGP responds to the jet.
- A significant evolution of R_{AA} with $\sqrt{d_{12}}$ is observed, at small $\sqrt{d_{12}}$ values, indicating a significant difference in the quenching of large-radius jets having single sub-jet and those with more complex substructure. No significant dependence of R_{AA} on $\sqrt{d_{12}}$ is observed at larger $\sqrt{d_{12}}$.
- Shadowing in nucleon-nucleon cross section in HI collisons might be a possible explanation of the underestimate of the measured Z/W boson yields in Pb+Pb by the nPDF predictions as well as the excess of W yields in peripheral collisions.
- The measured diphoton invariant mass distribution is used to set new exclusion limits on the production of axion-like particles.

More details and results from the heavy ion physics program realized by ATLAS are available on https://twiki.cern.ch/twiki/bin/view/AtlasPublic/HeavyIonsPublicResults

Thank you for your attention!

Backup slides

The ATLAS detector

Detector coverage:

Inner Detector (ID):

$|\eta| < 2.5$

Calorimeter (CAL):

$|\eta| < 3.2$ (EM)

$|\eta| < 4.9$ (HAD)

$3.2 < |\eta| < 4.9$ (FCal)

Muon Spectrometer (MS):

$|\eta| < 2.7$

Zero Degree Cal. (ZDC):

$|\eta| > 8.3 \quad @z = \pm 140$ m

MB Trig. Scint. (MBTS):

$2.1 < |\eta| < 3.9$

Magnetic fields:

- 2T solenoid field in ID
- Toroidal field in MS

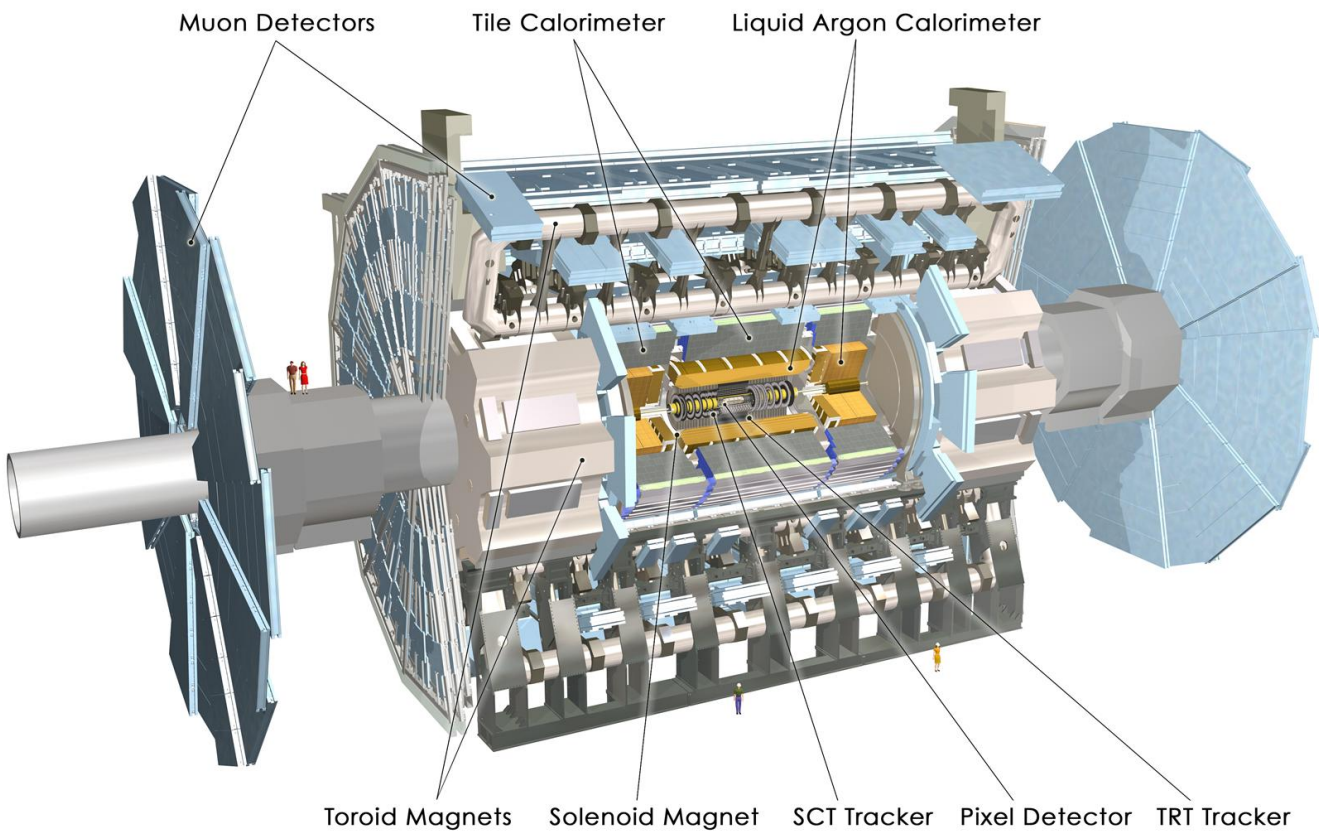

Identification of minimum-bias p+Pb and Pb+Pb collision measurement of spectator neutrons in ZDC and charged particle tracks (pulse hight and arrival times) in MBTS.

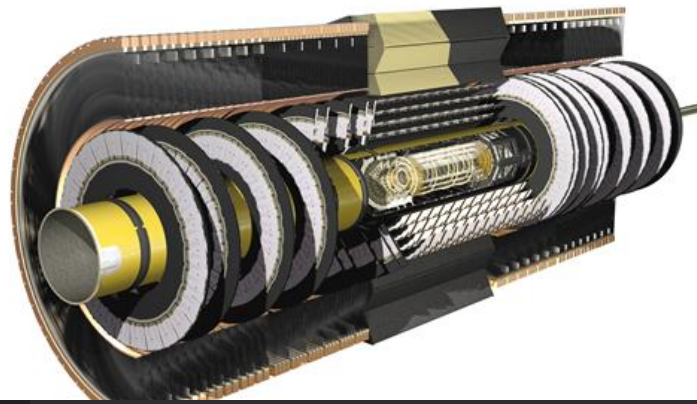

Nuclear modification factor R_{AA} for the inclusive jets

- The R_{AA} value is independent of rapidity at low jet p_{T}. For jets with $p_{\mathrm{T}} \gtrsim 300$ GeV a sign of a decrease with rapidity is observed.
- The magnitude of the R_{AA} as well as its evolution with jet p_{T} and rapidity are consistent with those reported in a similar measurement performed with Pb+Pb collisions at $\sqrt{s_{\mathrm{NN}}} = 2.76$ TeV in the overlapping kinematic region.

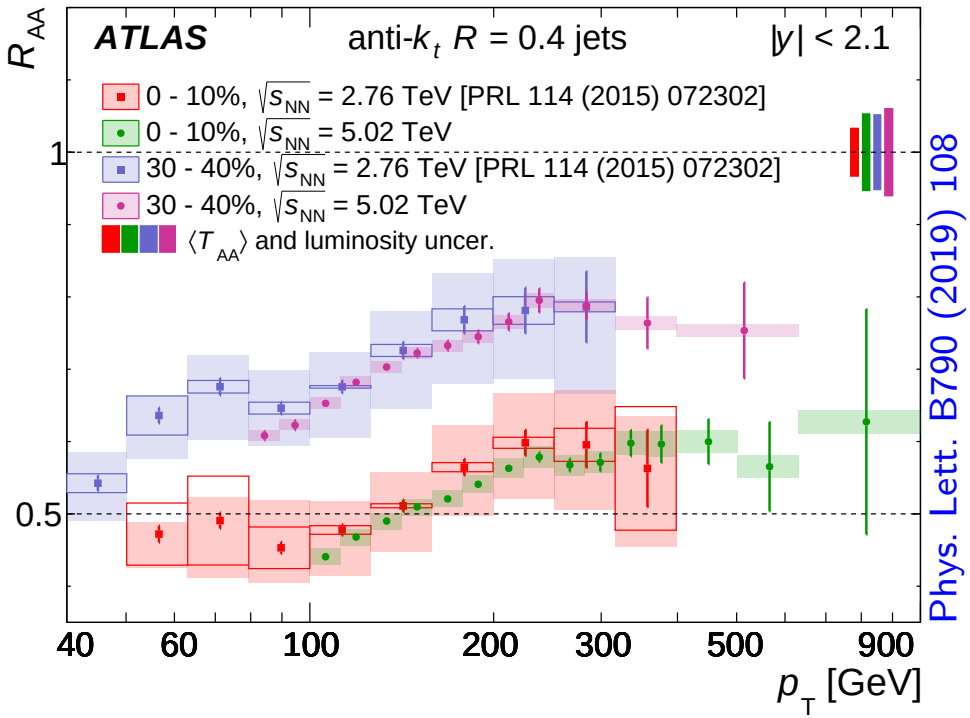

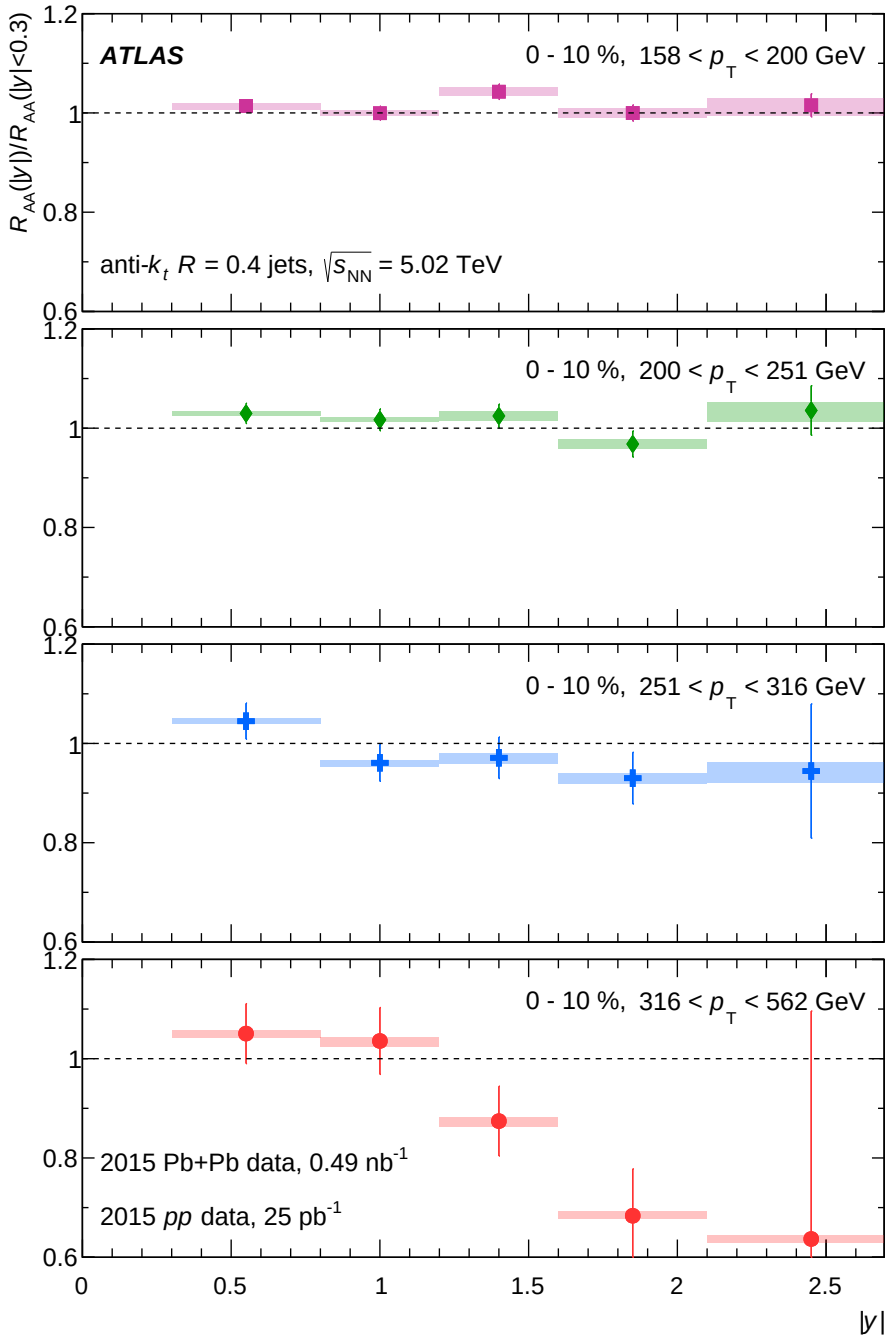

Charged-particle distributions within and around jet

- The observed behavior inside the jet cone, $r < 0.4$, agrees with the measurement of the inclusive jet fragmentation functions, where yields of fragments with $p_{\mathrm{T}} < 4$ GeV are observed to be enhanced and yields of charged particles with intermediate p_{T} are suppressed in Pb+Pb collisions compared to those in pp collisions.

PRC 98 (2018) 024908

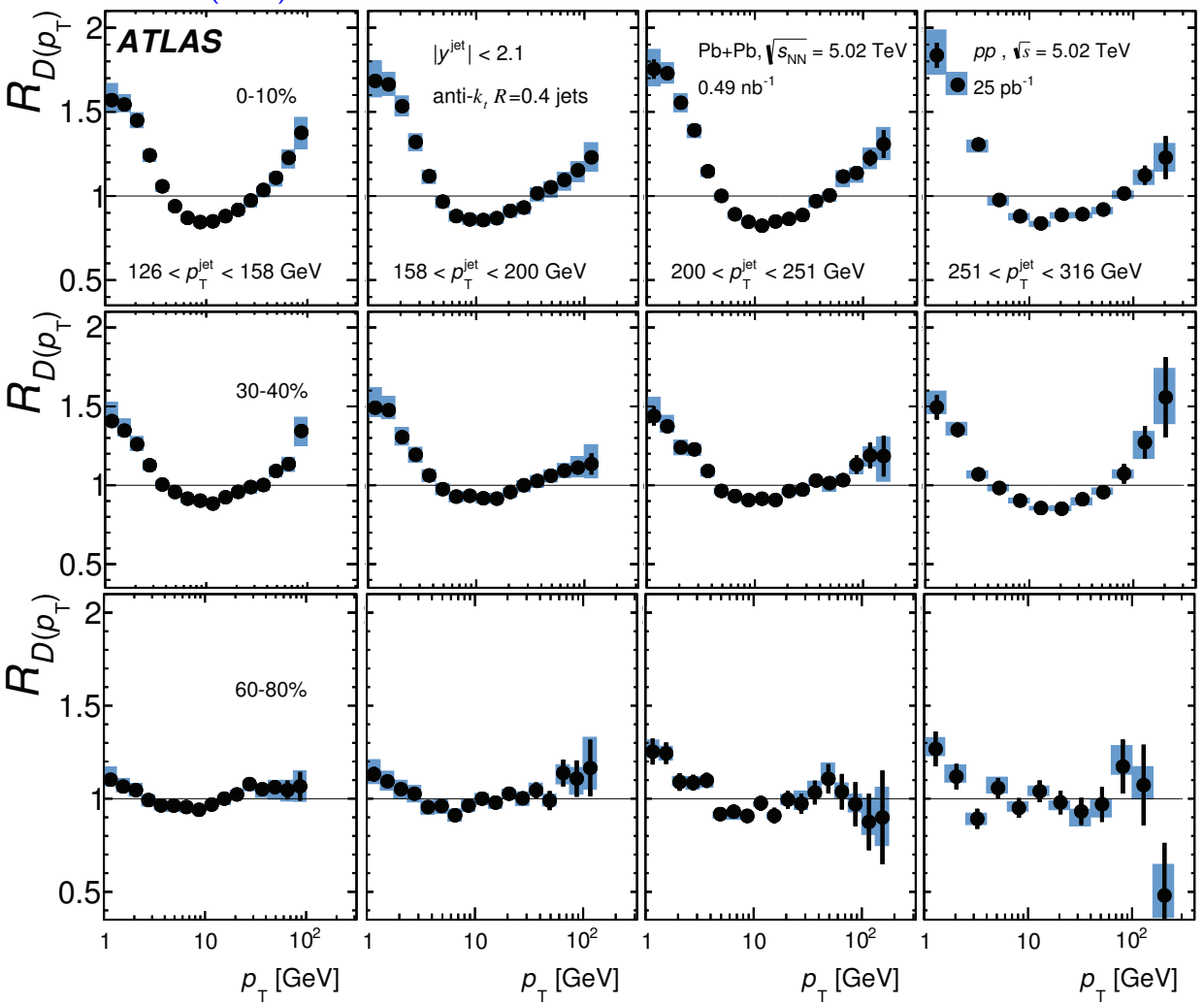

- $R_{D(p_{\mathrm{T}})} = \dfrac{D(p_{\mathrm{T}})_{\mathrm{Pb+Pb}}}{D(p_{\mathrm{T}})_{pp}}$
- $D(p_{\mathrm{T}}) = \dfrac{1}{N_{\mathrm{jet}}} \dfrac{dn_{\mathrm{ch}}}{dp_{\mathrm{T}}}$
- Excess of soft particles observed in central Pb+Pb collisions exhibits only a small $p_{\mathrm{T}}^{\mathrm{jet}}$ dependence.

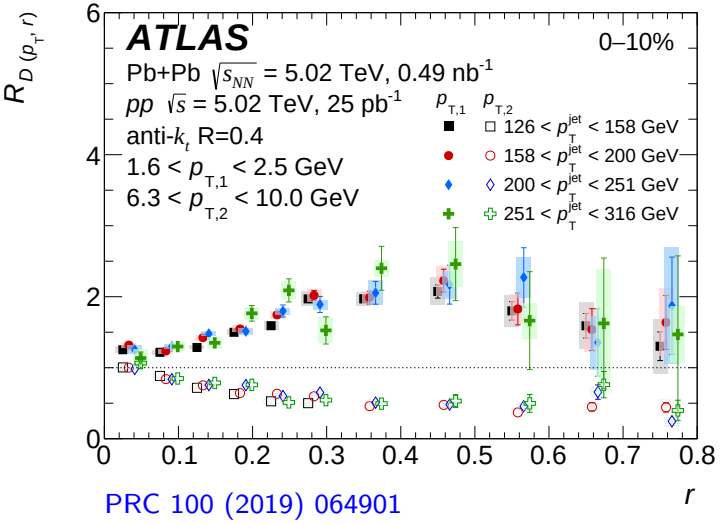

PRC 100 (2019) 064901

Ratios of yields integrated over p_{T} and r

- The yields integrated over the p_{T} range of $1-4$ GeV and distance r from the jet axis:

$$\Theta(r) = \int_{1\ \mathrm{GeV}}^{4\ \mathrm{GeV}} D(p_{\mathrm{T}}, r)\, dp_{\mathrm{T}} \qquad P(r) = \int_{0}^{r}\int_{1\ \mathrm{GeV}}^{4\ \mathrm{GeV}} D(p_{\mathrm{T}}, r')\, dp_{\mathrm{T}}\, dr'$$

provide a concise look at the enhancement region, using ratios:

$$R_{\Theta(r)} = \Theta(r)_{\mathrm{Pb+Pb}} \big/ \Theta(r)_{pp} \qquad R_{P(r)} = P(r)_{\mathrm{Pb+Pb}} \big/ P(r)_{pp}$$

- Most of the excess of charged-particles with p_{T} in the range $1-4$ GeV in Pb+Pb collisions is observed in the peripherals of the jets ($r \approx 0.4$).
- A significant $p_{\mathrm{T}}^{\mathrm{jet}}$ dependence is seen in the $R_{P(r)}$ distributions for the most-central Pb+Pb collisions.

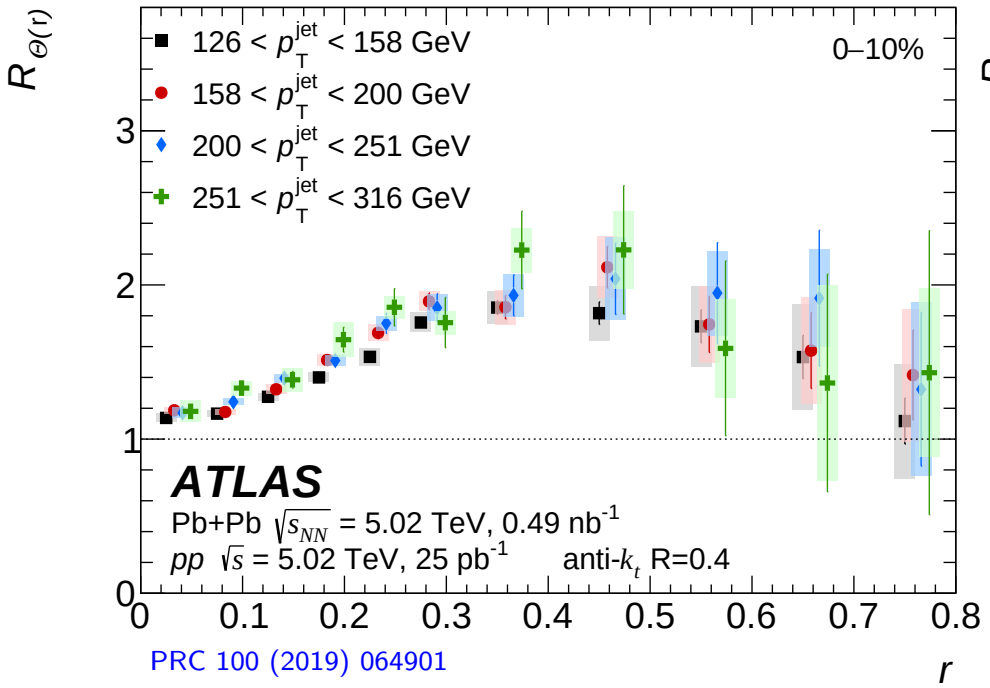

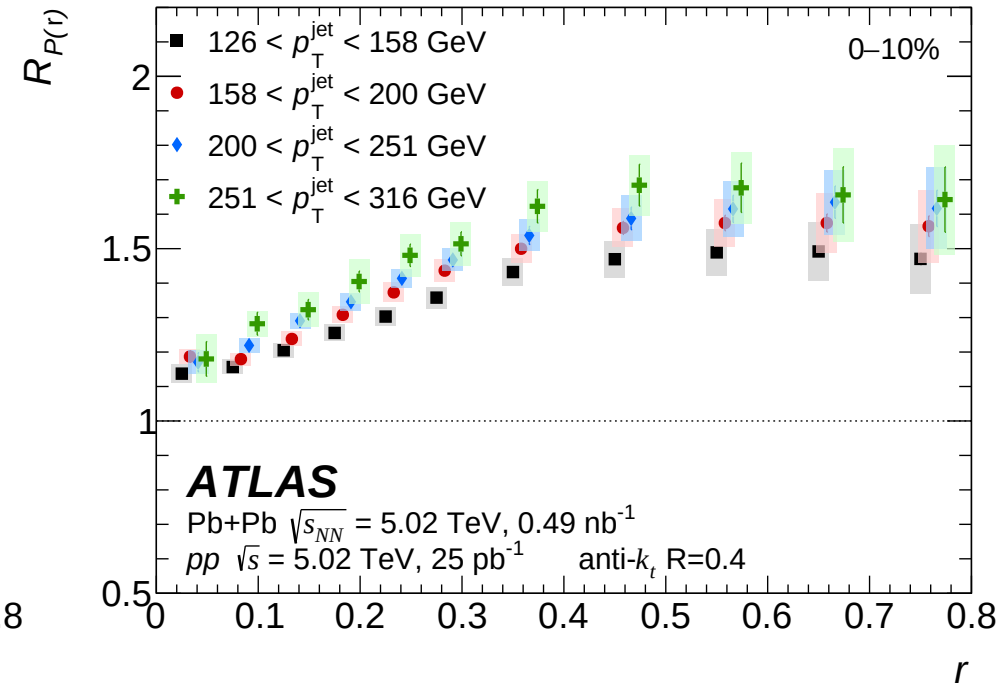

Suppression of large-radius jets

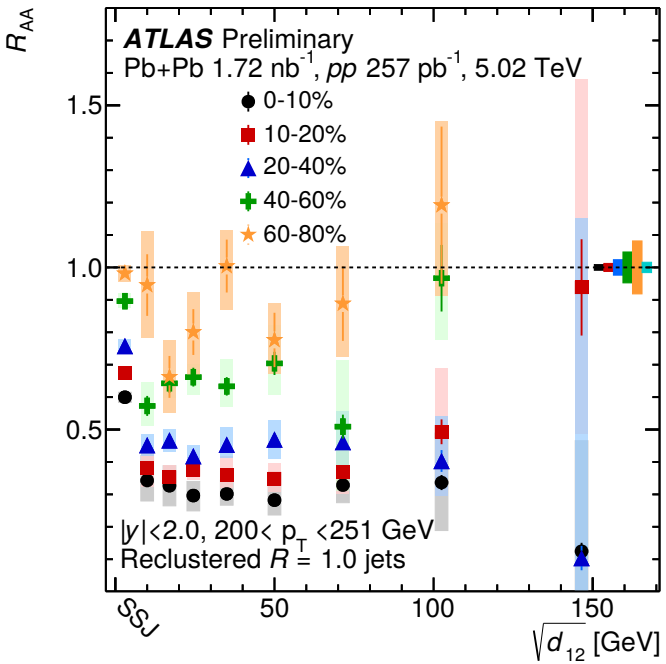

- Significantly different values of the R_{AA} for SSJ compared to jets with more complex sub-structure.
- R_{AA} sharply decreases with increasing $\sqrt{d_{12}}$ for small values of the splitting scale followed by flattening for larger $\sqrt{d_{12}}$.
- This is qualitatively consistent with the effects where the medium can not resolve partonic fragments below a certain transverse scale.

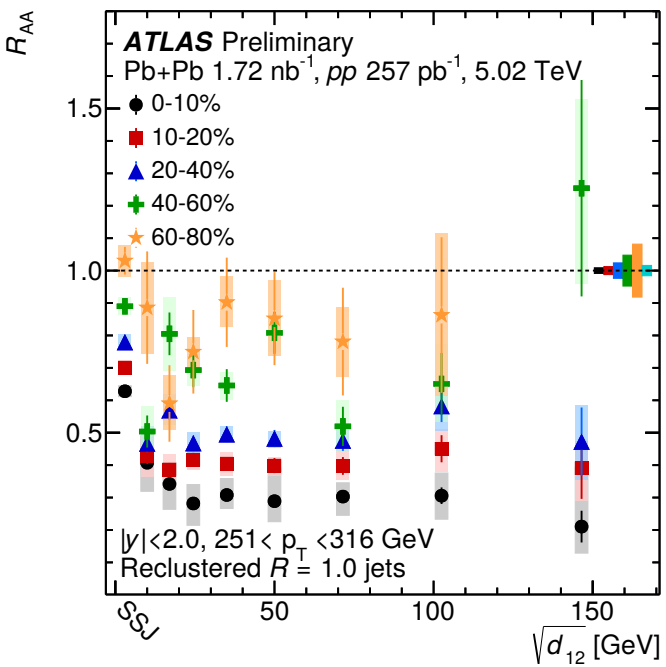

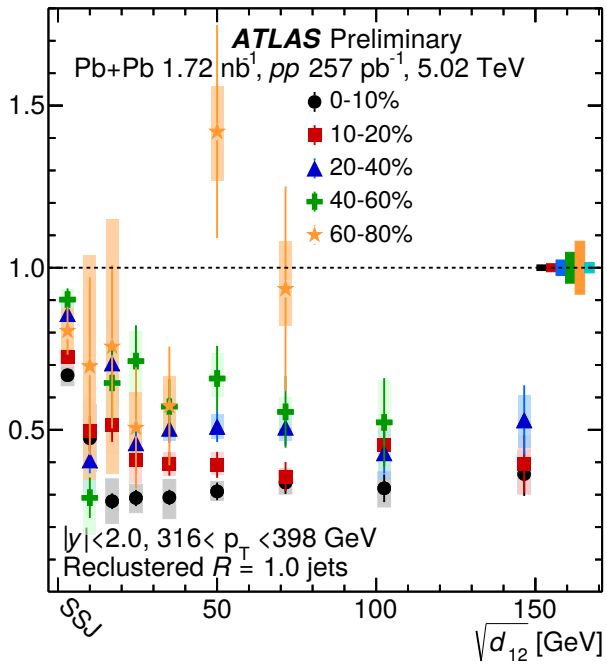

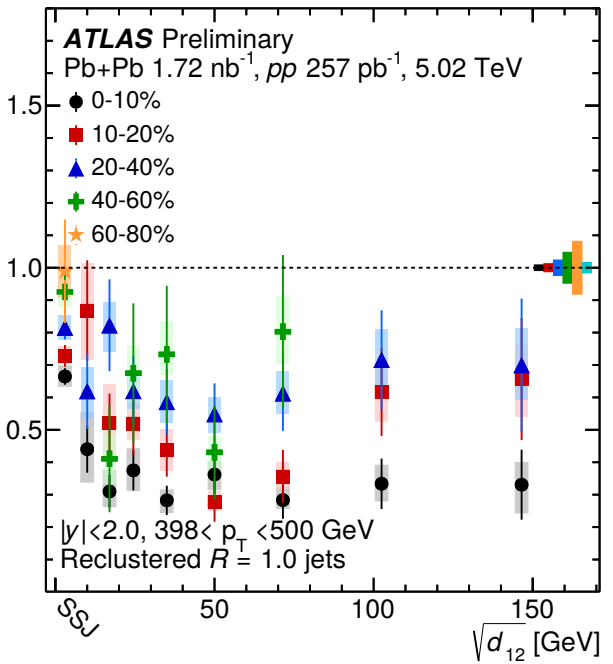

ATLAS-CONF-2019-056

Suppression of large-radius jets

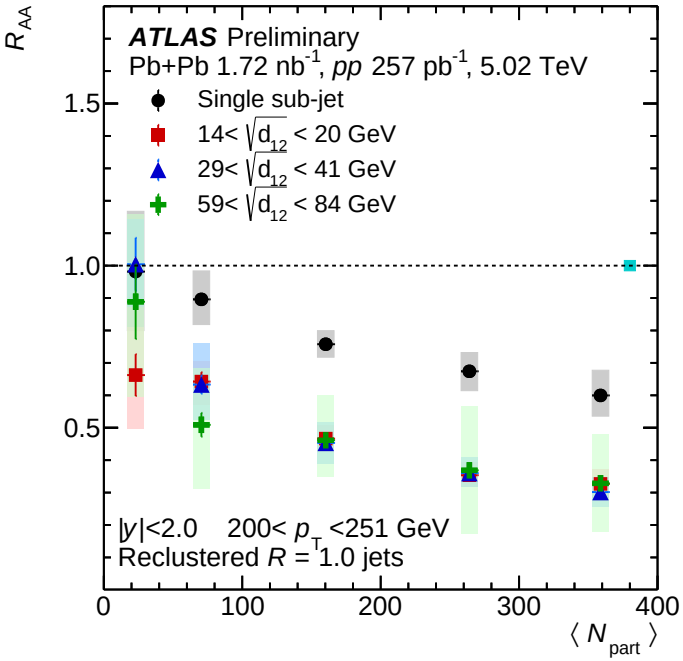

- Continous increase of the suppression with increasing centrality.
- The SSJ jets are less suppressed with respect to those with higher sub-jet multiplicity.

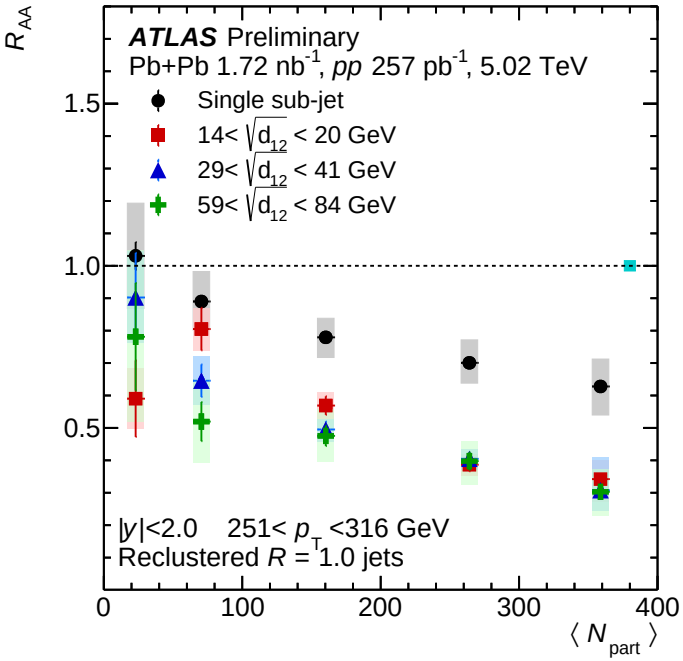

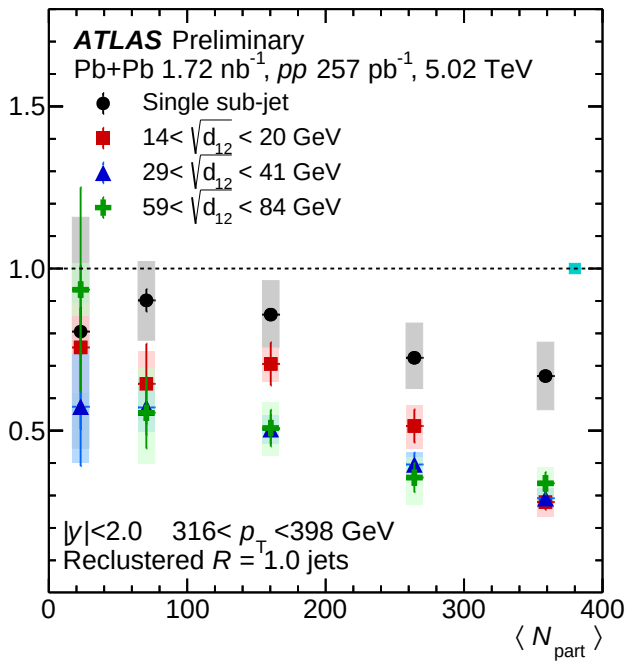

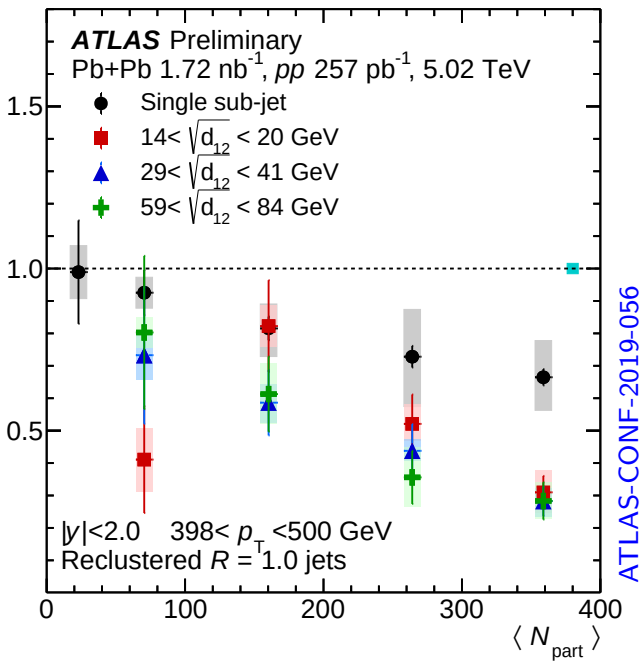

ATLAS-CONF-2019-056

Suppression of large-radius jets

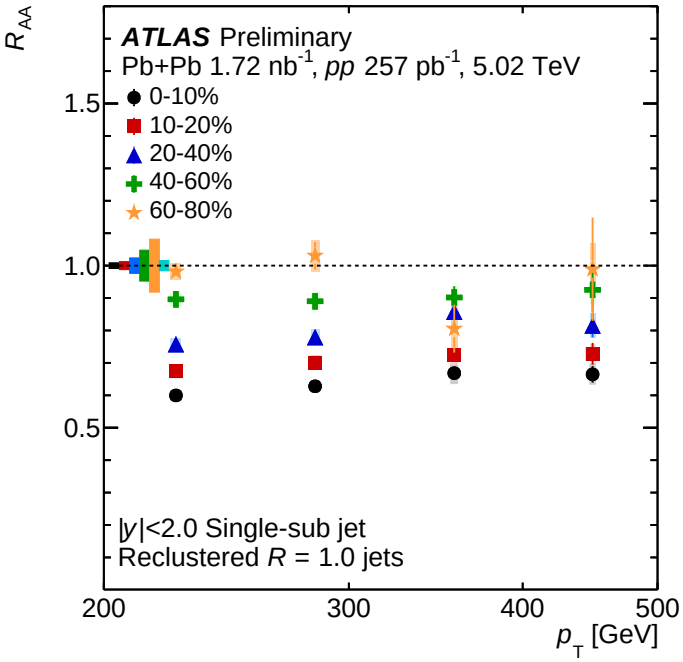

- For SSJ jets, R_{AA} grows slowly with increasing jet p_{T}.
- No significant p_{T} dependence of R_{AA} is observed for jets with multiple sub-jets.

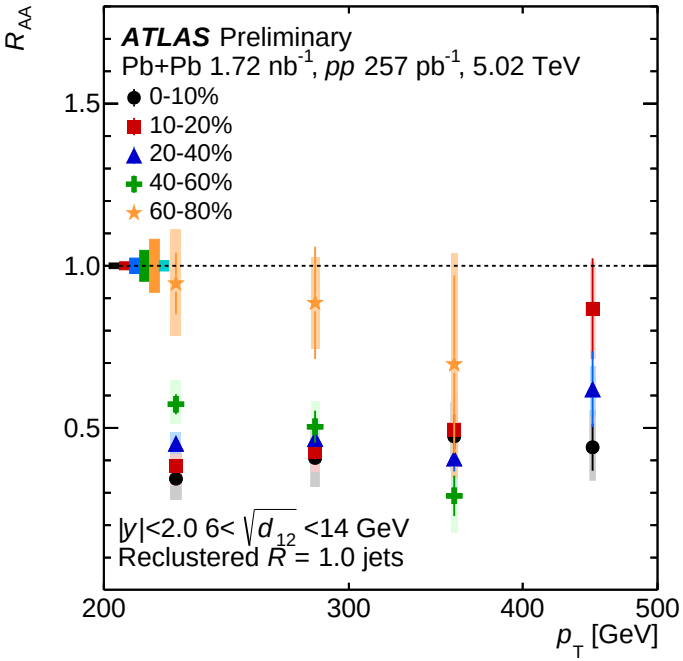

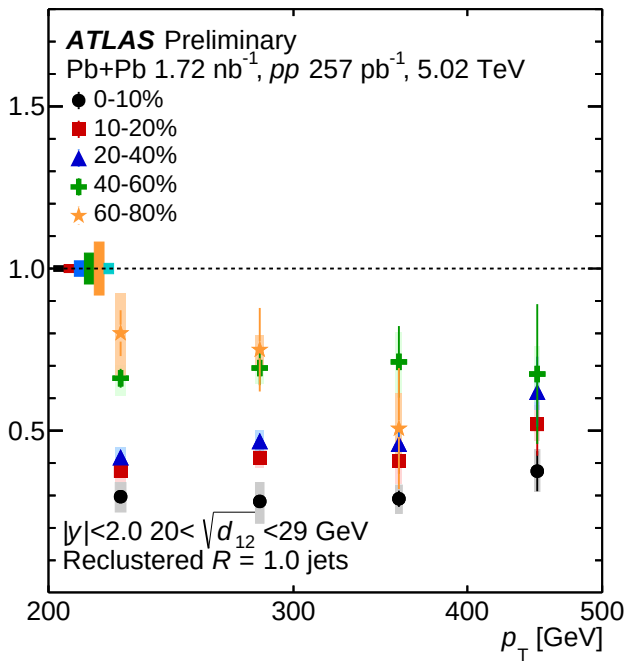

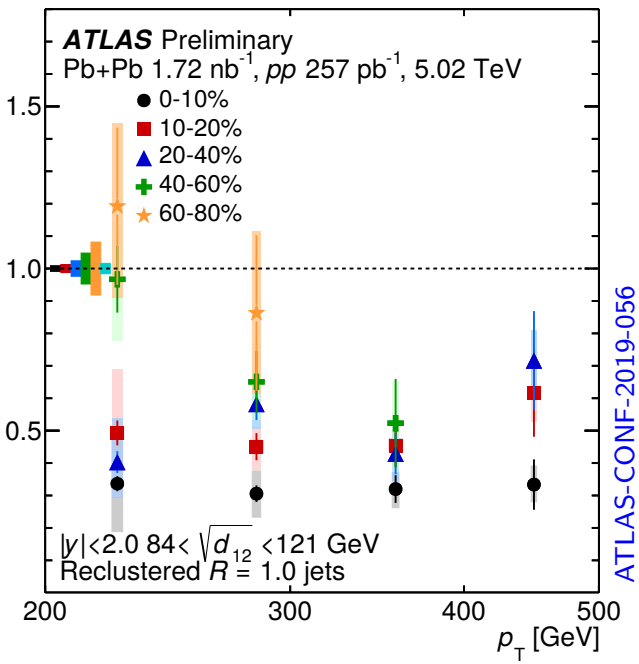

ATLAS-CONF-2019-056

Reconstruction of Z/W bosons with the ATLAS detector

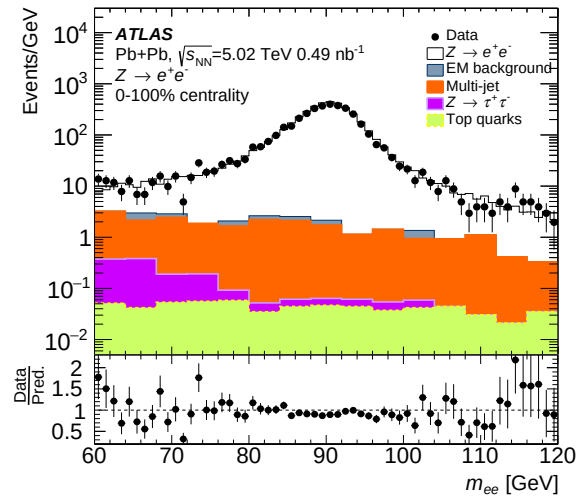

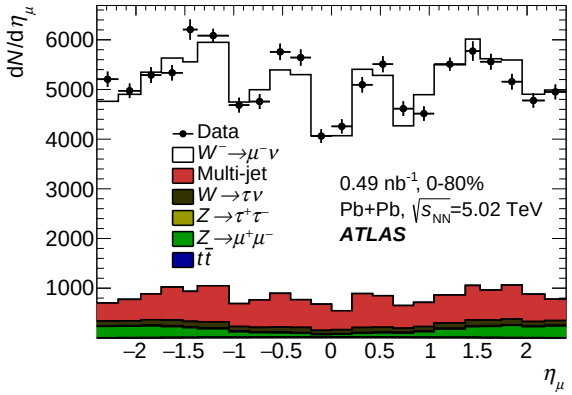

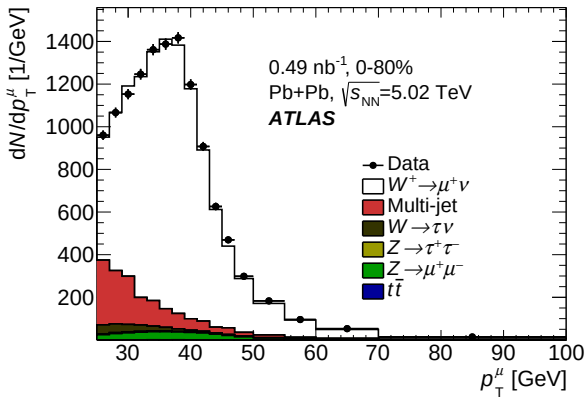

- Z/W bosons are measured in their leptonic ($\ell = e, \mu$) decay channels: $W^\pm \to \ell^\pm \overset{(-)}{\nu}$ and $Z \to \ell^+\ell^-$
- Events collected with single-lepton triggers:
  $p_{\mathrm{T}}^e > 15$ GeV and $p_{\mathrm{T}}^\mu > 14$ GeV
- High quality reconstruction and isolation (minimize hadronic activity around) requirements on the leptons.
- Final kinematic selection cuts on Z/W bosons:
  $|\eta_e| < 1.37, \quad 1.52 < |\eta_e| < 2.47, \quad |\eta_\mu| < 2.4$

  Specific cuts for Z boson selection:
  - opposite charge leptons with $p_{\mathrm{T}}^\ell > 20$ GeV,
  - invariant mass $66 < m_{\ell\ell} < 116$ GeV.

  Specific cuts for $W^\pm$ boson selection:
  - $p_{\mathrm{T}}^\ell > 25$ GeV, $\quad p_{\mathrm{T}}^{\mathrm{miss}} > 25$ GeV,
  - $m_{\mathrm{T}} = \sqrt{2 p_{\mathrm{T}}^\ell p_{\mathrm{T}}^{\mathrm{miss}} (1 - \cos\Delta\phi)} > 40$ GeV,
  - veto on Z events: $m_{\ell\ell} < 66$ GeV, with $p_{\mathrm{T},2}^\ell > 20$ GeV.
- Multi-jet bkgr. (semileptonic decays of HF, decays of K-s and π-s in muon channel, photon conversions, misidentified hadrons, ...) - estimated from data using template fits.

Z/W boson production in pp collisions at $\sqrt{s} = 5.02$ TeV

Fiducial integrated and differential cross sections measured in pp collisions serve as a reference for Pb+Pb interactions.

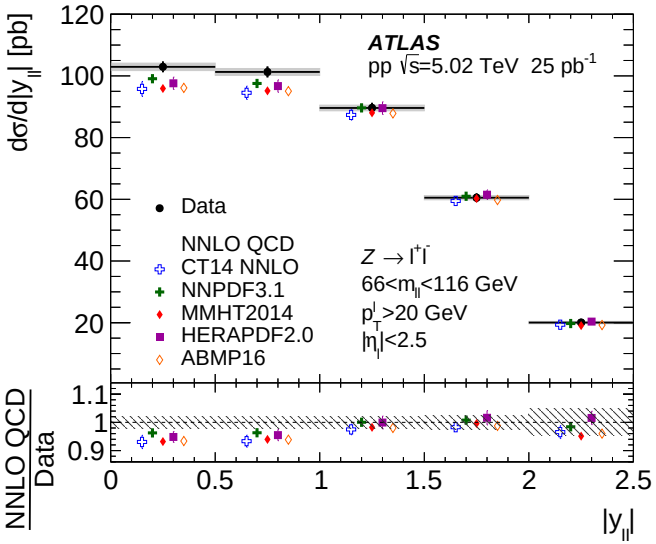

EPJC 79 (2019) 128

- Separate measurements in e and μ decay channels.
- Combined integrated fiducial cross sections:

$$W^+ : \quad 2266 \pm 9\ (\text{stat}) \pm 29\ (\text{sys}) \pm 43\ (\text{lumi})\ \text{pb}$$
$$W^- : \quad 1401 \pm 7\ (\text{stat}) \pm 18\ (\text{sys}) \pm 27\ (\text{lumi})\ \text{pb}$$
$$Z : \quad 374.5 \pm 3.4\ (\text{stat}) \pm 3.6\ (\text{sys}) \pm 7.0\ (\text{lumi})\ \text{pb}$$

- Overall good agreement with NNLO pQCD calculations.
- $A_\ell = \dfrac{\mathrm{d}N_{W^+\to\ell^+\nu_\ell}/\mathrm{d}\eta_\ell \ - \ \mathrm{d}N_{W^-\to\ell^-\bar{\nu}_\ell}/\mathrm{d}\eta_\ell}{\mathrm{d}N_{W^+\to\ell^+\nu_\ell}/\mathrm{d}\eta_\ell \ + \ \mathrm{d}N_{W^-\to\ell^-\bar{\nu}_\ell}/\mathrm{d}\eta_\ell}$

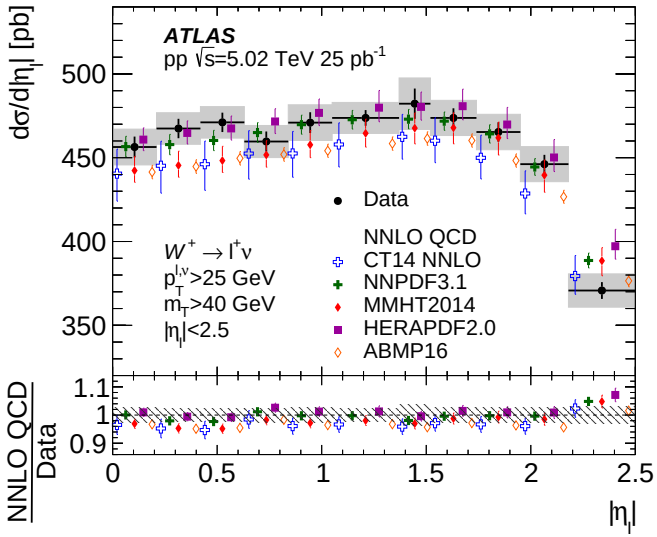

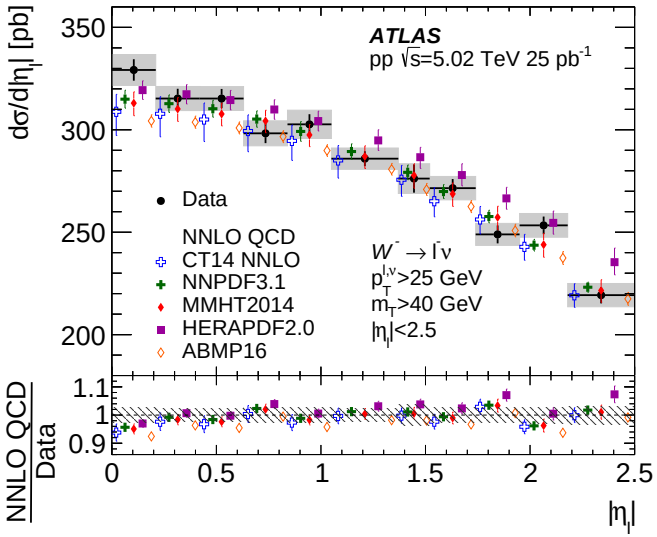

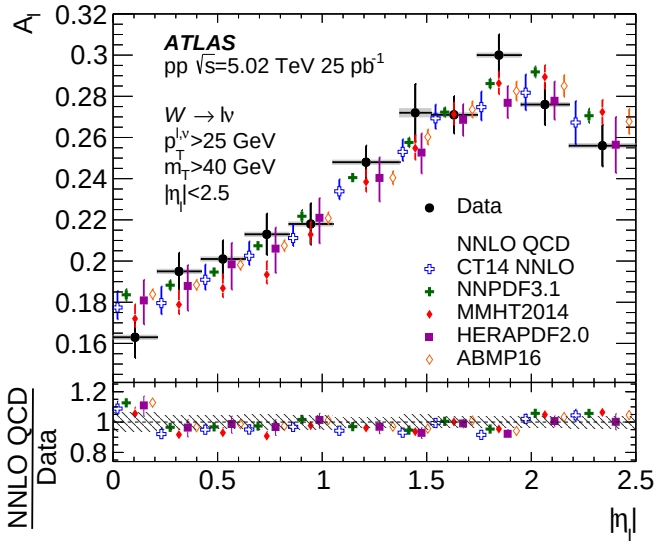

Binary scaling - Glauber MC comparison

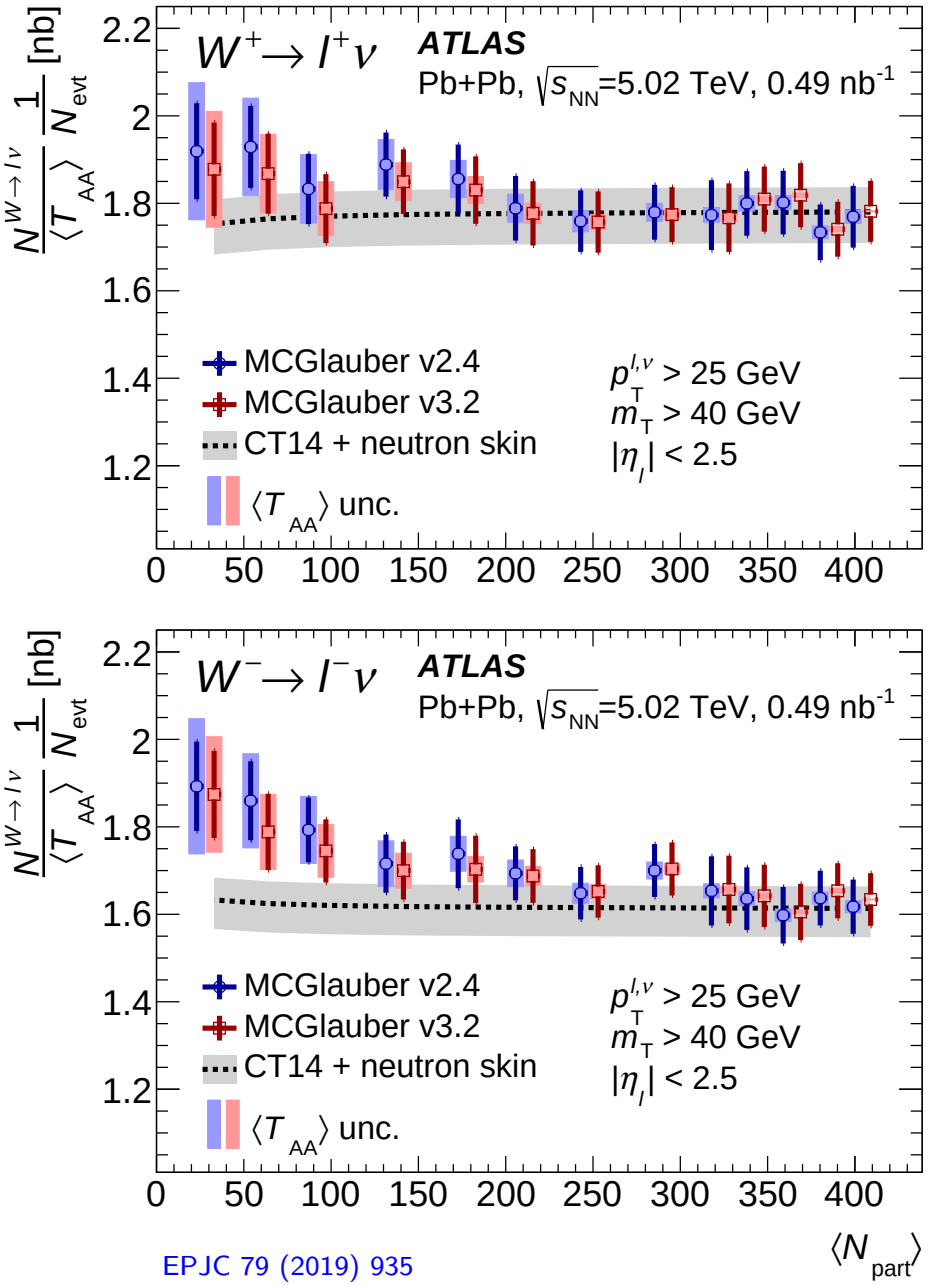

EPJC 79 (2019) 935

- Comparison of Glauber MC v2.4 and v3.2 (includes different radial distributions of p and n in nuclei, which results in an evolution of the effective p/n ratio with centrality).
- No significant change of the measured yields.
- Theory curves obtained using the CT14 NLO PDF set include the neutron skin effect included in Glauber MC v3.2.
- Slopes of Z boson R_{AA} vs. $\langle N_{\mathrm{part}} \rangle$:
  Glauber v2.4: $(10 \pm 7)\%$; v3.2: $(5 \pm 6)\%$

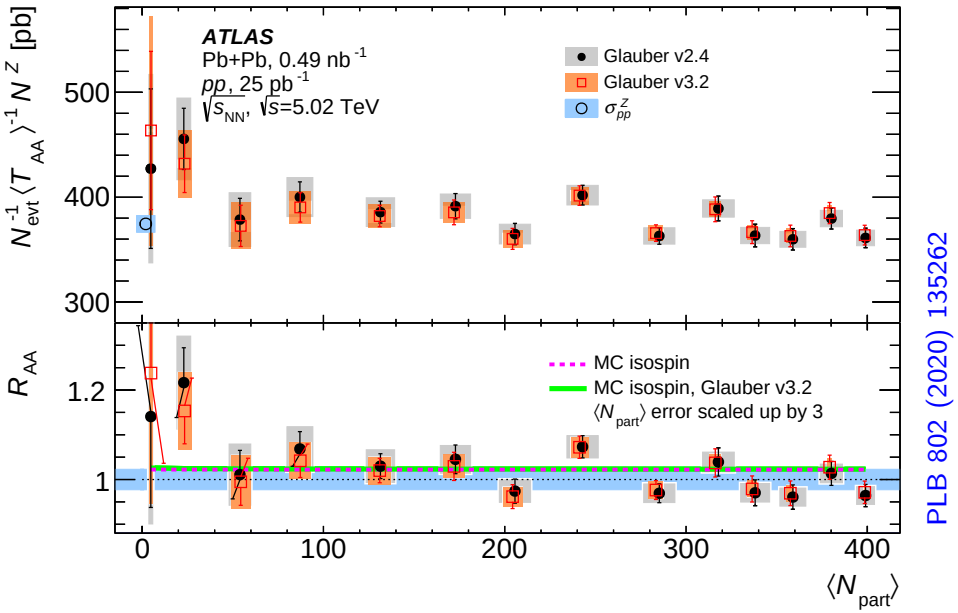

PLB 802 (2020) 135262

Comparison with HG-Pythia predictions

- Peripheral decrease in production yield predicted by HG-PYTHIA (PLB773 (2017) 408)
- In qualitative agreement with charged hadrons R_{AA} suppression observed by ALICE.
- Opposite trends observed by ATLAS in Z and W boson yields.
- Theoretical predictions are calculated with the CT14 NLO PDF set multiplied by the R_{AA} obtained from HG-PYTHIA.

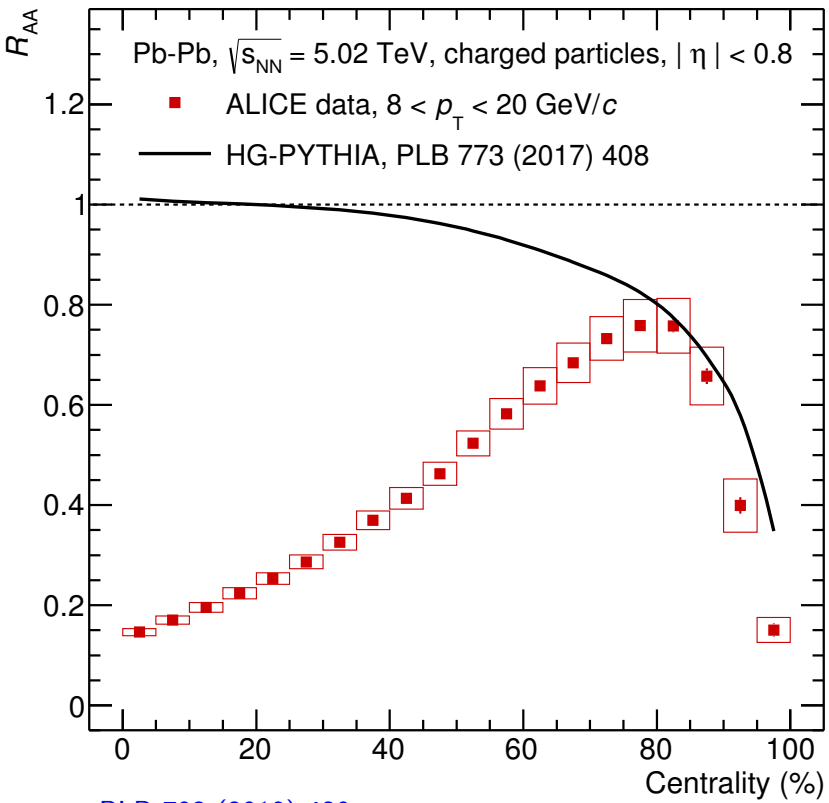

PLB 793 (2019) 420

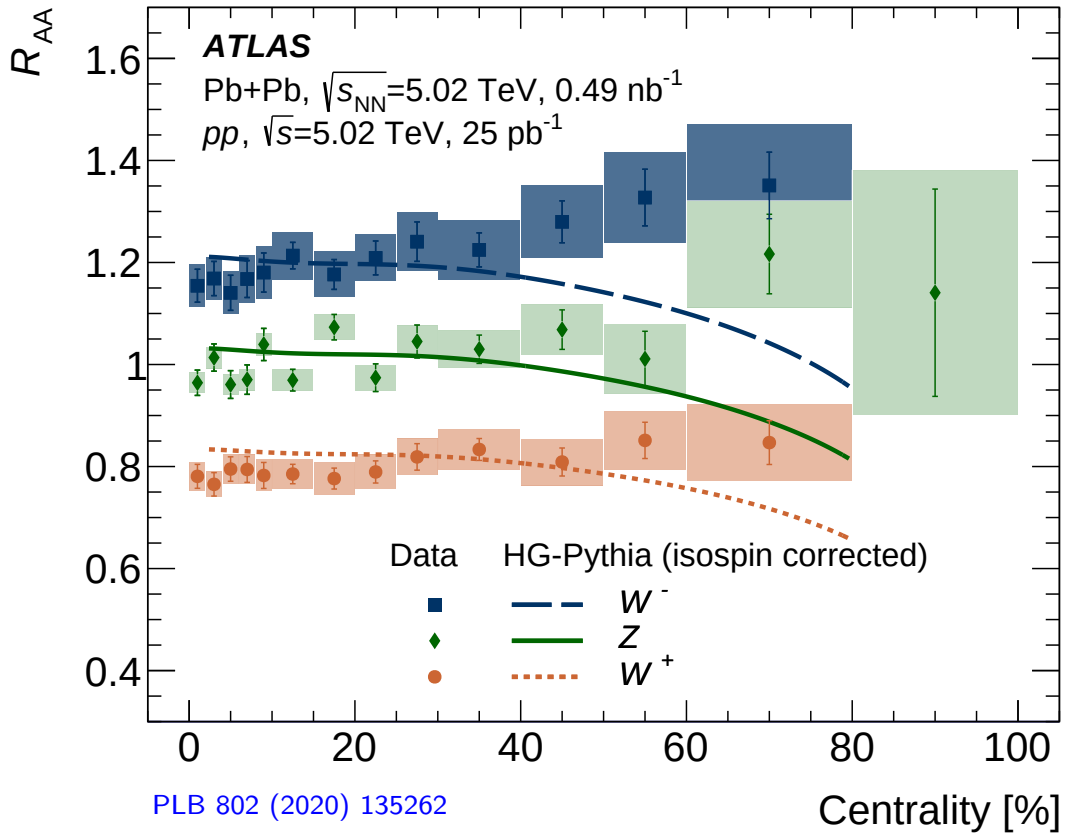

PLB 802 (2020) 135262